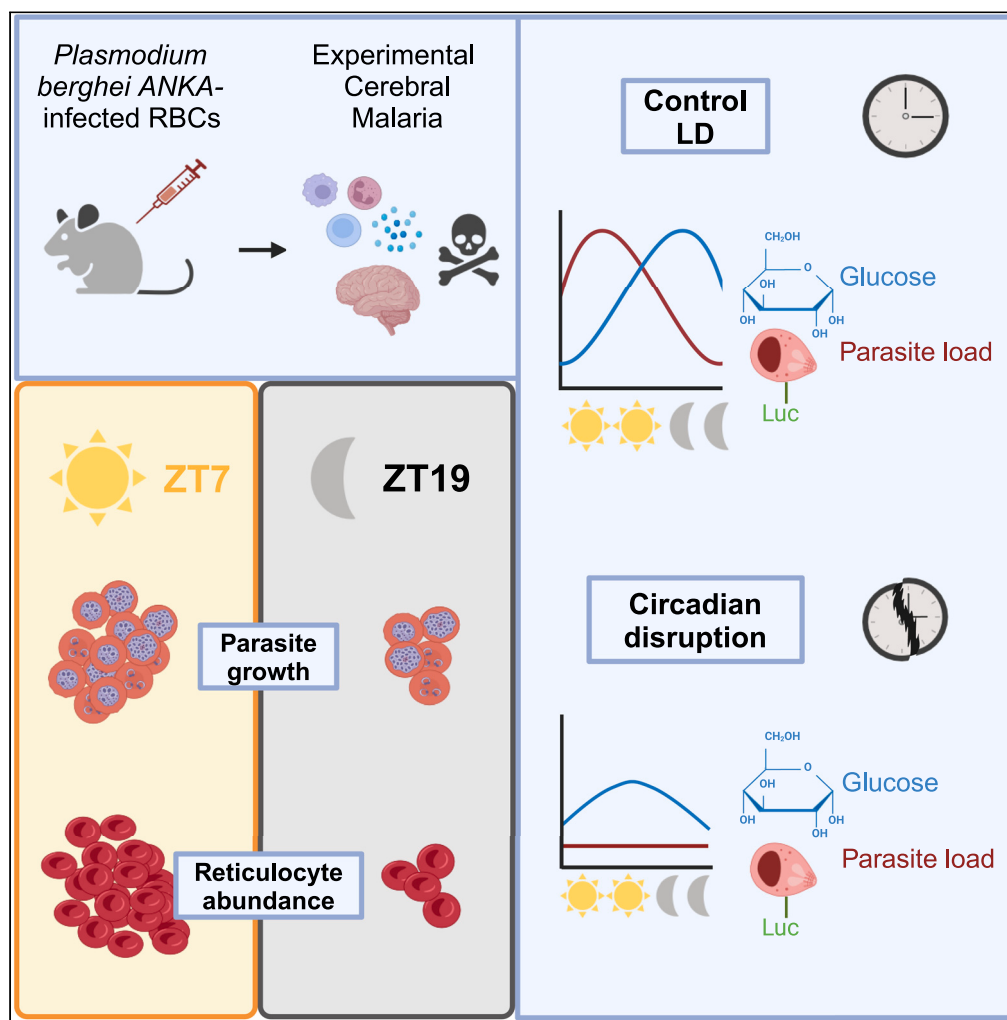


Article

Time of day and circadian disruption influence host response and parasite growth in a mouse model of cerebral malaria



Priscilla Carvalho Cabral, Joelle Weinerman, Martin Olivier, Nicolas Cermakian

nicolas.cermakian@mcgill.ca

Highlights

Time of infection influences malaria parasite growth and host response in mice

Reticulocyte levels *in vivo*, and the level of infection, vary over 24 h

Environmental circadian disruption impairs parasite growth *in vivo*

Parasite rhythmicity is affected by host metabolism, in particular glucose

Carvalho Cabral et al., iScience 27, 109684 May 17, 2024 © 2024 The Author(s). Published by Elsevier Inc. <https://doi.org/10.1016/j.isci.2024.109684>



Article

Time of day and circadian disruption influence host response and parasite growth in a mouse model of cerebral malaria

Priscilla Carvalho Cabral,^{1,2} Joelle Weinerman,¹ Martin Olivier,^{2,3} and Nicolas Cermakian^{1,4,*}

SUMMARY

Malaria is a disease caused by infection with parasite *Plasmodium* spp. We studied the circadian regulation of host responses to the parasite, in a mouse model of cerebral malaria. The course of the disease was markedly affected by time of infection, with decreased parasitemia and increased inflammation upon infection in the middle of the night. At this time, there were fewer reticulocytes, which are target cells of the parasites. We next investigated the effects of desynchronization of host clocks on the infection: after 10 weeks of recurrent jet lags, mice showed decreased parasite growth and lack of parasite load rhythmicity, paralleled by a loss of glucose rhythm. Accordingly, disrupting host metabolic rhythms impacted parasite load rhythmicity. In summary, our findings of a circadian modulation of malaria parasite growth and infection shed light on aspects of the disease relevant to human malaria and could contribute to new therapeutic or prophylactic measures.

INTRODUCTION

Circadian rhythms are defined as physiological and behavioral oscillations with a period of approximately 24 h, matching the Earth's rotation, that persist in the absence of environmental timing cues. These rhythms are regulated by a master pacemaker located in the suprachiasmatic nucleus in the brain as well as clocks located in most other tissues and cell types throughout the organism. Many organisms' bodily functions, such as temperature regulation, levels of activity, and hormonal secretion, are known to be under circadian control.¹ In particular, circadian rhythms in immunity (cytokine/chemokine regulation, cell expansion, and humoral/cellular responses) have been widely reported.^{2–5} This has important consequences for host susceptibility to infections depending on the time of the day the host encounters the pathogen.^{6,7}

Indeed, rhythms in host response to infections have been reported,^{8–10} and in many cases, these occur as a direct consequence of rhythmic immune responses.¹¹ This is the case for parasitic infections such as leishmaniasis: mice infected with *Leishmania major* promastigotes at the beginning of the subjective day showed reduced inflammation at the site of inoculation and lower parasite load when compared to mice infected at the end of the subjective day.^{11,12} Notably, the clock within immune cells was controlling the magnitude of *L. major* infection, impacting chemoattractant expression and innate cell recruitment.¹¹ In a model of parasitic worm infection, it was shown that infection in the early night resulted in a decreased Th2 response and a higher parasite burden 21 days post-infection, in comparison to early-day infected mice.¹³

Despite these few reports, the mechanisms driving the rhythms in susceptibility to infections, especially in parasitic diseases, remain largely unknown. One parasitic disease with a daily component is malaria, a vector-transmitted disease caused by *Plasmodium* spp. parasites affecting hundreds of millions of people around the globe.¹⁴ In some cases, mostly in children, this infection can lead to severe immune responses resulting in multi-organ damage and death. Fevers often occur in rhythms of 24 h or multiples, and the replication cycle of the parasite inside the host target cells (red blood cells, RBCs) follows a daily rhythm.^{15–17} Moreover, the time of day at which the *Anopheles* mosquito bites the host and transmits the sporozoite form of the parasite matters for transmission success.^{18–20} However, it remains to be investigated, during malaria intraerythrocytic stage of the disease, if the time of day at which hosts encounter malaria parasite blood stages can also impact the progression of the disease.

Host metabolism and timing of host feeding were shown to be important in regulating *Plasmodium chabaudi* rhythmic replication cycle,^{21,22} although contrasting results have been reported.²³ More specifically, the phase of the parasite replication cycle was inverted when mice were fed in the daytime instead of their usual mostly nocturnal feeding.²¹ Parasite proliferation rhythms were aligned with the timing of host food intake when levels of plasma glucose were highest.²² Furthermore, endogenous IFN γ was responsible for regulating

¹Douglas Research Centre, McGill University, Montréal, QC H4H 1R3, Canada²Department of Microbiology and Immunology, McGill University, Montréal, QC H3A 2B4, Canada³Research Institute of the McGill University Health Centre, Montréal, QC H4A 3J1, Canada⁴Lead contact

*Correspondence: nicolas.cermakian@mcgill.ca

<https://doi.org/10.1016/j.isci.2024.109684>

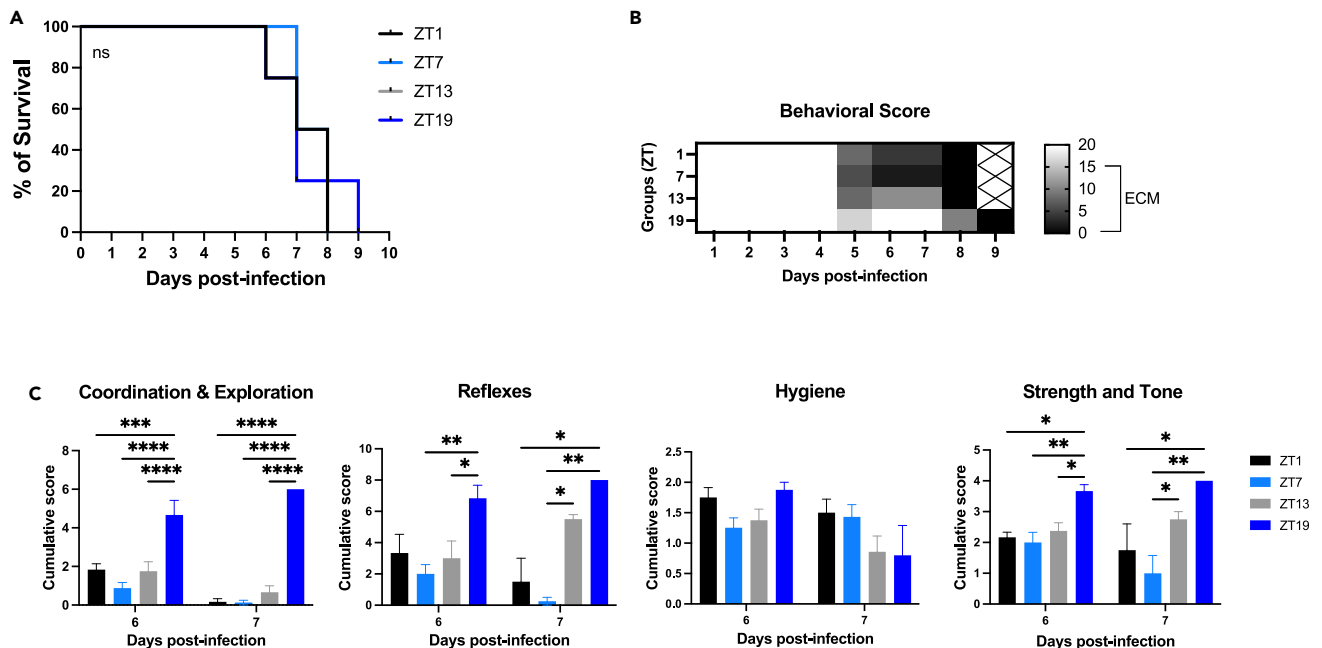


Figure 1. Host survival and sickness behavior in response to *Plasmodium berghei* ANKA infection

Mice were injected with *Plasmodium berghei* ANKA-infected erythrocytes at ZT1, 7, 13, or 19.

(A) Survival curve. Log rank (Mantel-Cox) test analysis, ns.

(B) Experimental cerebral malaria (ECM) behavioral score over days. A score equal to or below 15 is interpreted as ECM. The "X" mark indicates an absence of the dataset (no more mice alive).

(C) Group criteria assessment of infected mice.

Data are from one of three independent experiments performed, all with similar results, with 8 mice per group in each. Data are shown as mean \pm SEM. Mixed-effects model (REML) with Tukey's multiple comparisons test. * $p < 0.05$, ** $p < 0.01$, *** $p < 0.001$, **** $p < 0.0001$. See also [Figures S1, S3, and S4](#).

energy and glycolysis in leukocytes. The lack of this cytokine impaired TNF- α production while culminating in a loss of the 24 h rhythms in parasite replication forms.²²

To date, most work on daily rhythms in malaria has been done using *P. chabaudi*. In this model, circadian misalignment between the mouse host and the parasite negatively impacts parasite growth and virulence.^{24,25} Given that host rhythms can impact malaria parasite proliferation and the establishment of infection, it is logical to expect that the time at which hosts encounter parasites (time of infection) should also be a significant factor.

Furthermore, the immune activation component of this disease can result in fatal cases attributed to cerebral malaria.²⁶ To understand the mechanisms underlying this serious outcome, a mouse model of experimental cerebral malaria (ECM) is widely used,^{27,28} using the *Plasmodium berghei* ANKA strain, closely recapitulating the symptoms and pathogenesis of the human disease.²⁹

Here, we aimed to study the circadian regulation of *Plasmodium* infection in mice. We took advantage of the ECM model and *P. berghei* ANKA to study the phase of the disease that follows infected RBC disruption and subsequent activation of the host's immune response. We observed that time of infection influences host response and disease progression, with mice infected in the middle of the night showing parasite growth impairments, paralleled by reduced levels of infected reticulocytes. Moreover, similar parasite growth impairments were observed in mice subjected to chronic circadian disruption, clock mutant mice, and under experimental protocols of host metabolism disruption (time-restricted feeding and sucrose administration).

RESULTS

The time of day of infection impacts sickness behavior and immune response, but not survival, in a mouse model of cerebral malaria

To investigate if the time of infection dictates host susceptibility to cerebral malaria, mice were injected with *P. berghei* ANKA-infected erythrocytes (iRBCs) at either zeitgeber time (ZT) 1 (beginning of the day), ZT7 (middle of the day), ZT13 (beginning of the night), or ZT19 (middle of the night). All mice were infected using the same batch of iRBCs at the same time, so any effects would be due to the host time and not to parasite development stage rhythms or parasite-intrinsic rhythms. Mice were monitored for clinical scores of ECM and survival. We observed that regardless of the time of infection, all mice succumbed to the infection within days 6–9 post-infection (log rank test, $p = 0.9700$) (Figure 1A), an expected range for ECM.³⁰ ECM was confirmed by Evans blue dye incorporation in the brain of ECM-affected mice as a result blood-brain barrier disruption (Figure S1A). Up to day 6 post-infection, all mice had scored above 15 (no cerebral malaria), and as the infection progressed,

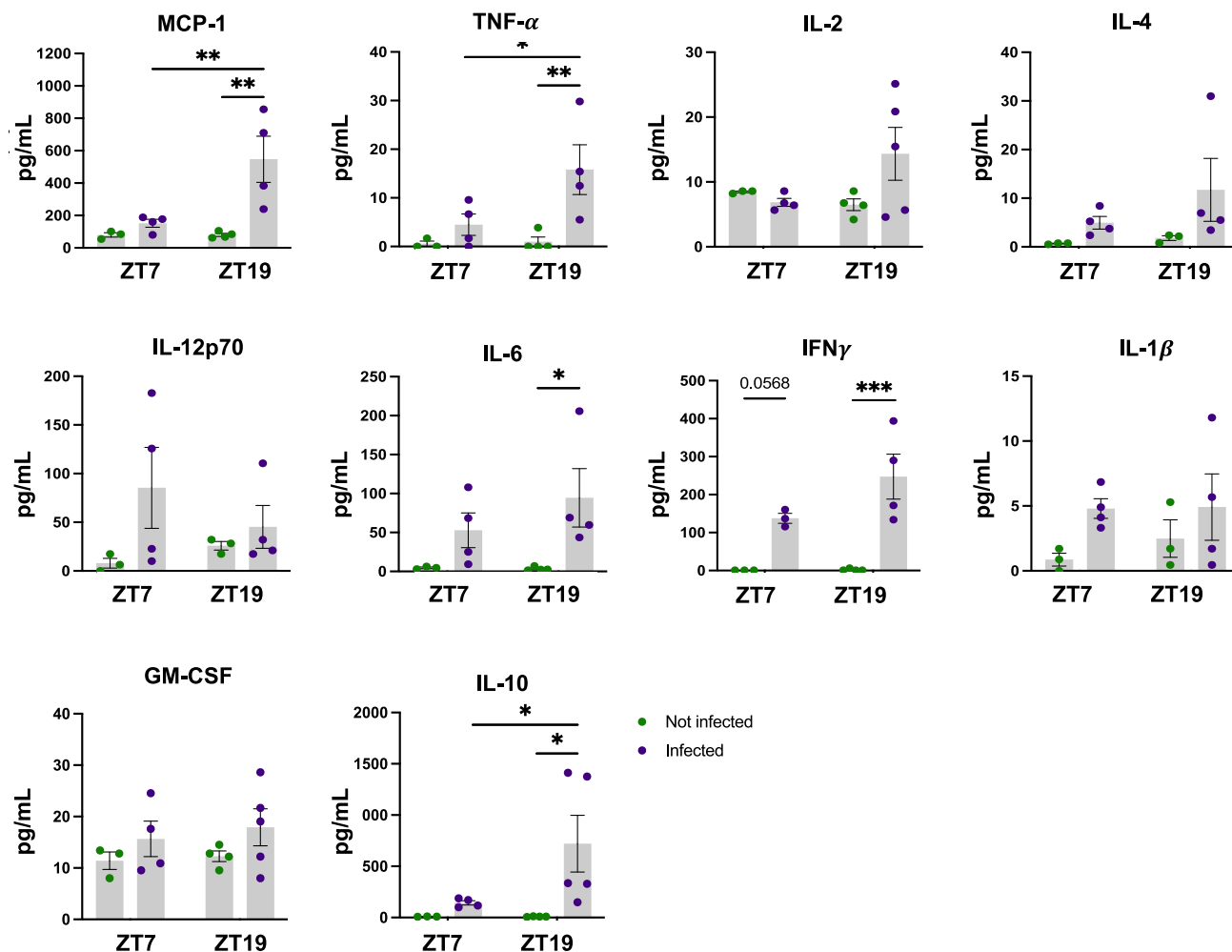


Figure 2. Host immune response to *Plasmodium berghei* ANKA is affected by the time of infection

Mice were injected with *Plasmodium berghei* ANKA-infected erythrocytes (infected) or saline (not infected) at ZT7 or ZT19. Blood was collected on day 6 post-infection and the levels of cytokine/chemokines were quantified in the serum, by multiplex array. 3–4 mice per group. Data are shown as mean \pm SEM. Two-way ANOVA with Sidak multiple comparisons test. * $p < 0.05$, ** $p < 0.01$, *** $p < 0.001$. See also [Figure S1](#).

most mice of all groups (except ZT19) had scores under 15 (i.e., cerebral malaria) ([Figure 1B](#)). This is not unexpected, as the clinical course of ECM is known to occur very quickly once the neurological stage of the disease has begun.^{31,32} When the criteria for the behavioral evaluation were analyzed separately, ZT19 mice scored higher in the coordination and exploration, reflexes, and strength and tone parameters ([Figure 1C](#)), indicating that the global sickness behavior was milder within this group. Nevertheless, ZT19 mice eventually underwent ECM and by day 9 post-infection, they had succumbed to the infection.

As the *P. berghei* ANKA is known to induce strong inflammatory responses during the course of the disease,^{30,33–35} we evaluated the levels of 10 cytokines and chemokines in the blood (serum) of mice infected at ZT7 or ZT19 on day 6 post-infection ([Figure 2](#)). Interestingly, overall there was a stronger inflammatory response to infection at ZT19 than at ZT7. Five of the cytokines/chemokines were significantly induced by infection exclusively in ZT19-infected mice (IL-10, TNF- α , MCP-1, IL-6, IFN γ), and none were induced significantly in ZT7-infected mice, although a trend can be observed for some proteins, such as for IFN γ ([Figure 2](#)).

Taken together, our data showed that in a mouse model of ECM, the time of infection affects the host inflammatory response and the development of ECM, without affecting survival.

The time of day of infection affects parasite growth and cell invasion

Given the time-dependent differences in the appearance of clinical features, we looked at parasite growth using two complementary methods: parasitemia (the proportion of RBCs that contain parasites, i.e., RBC with one or many parasites would have the same weight in the analysis) and parasite load (via bioluminescence measurements, so this measure is equivalent to the total amount of parasites in the

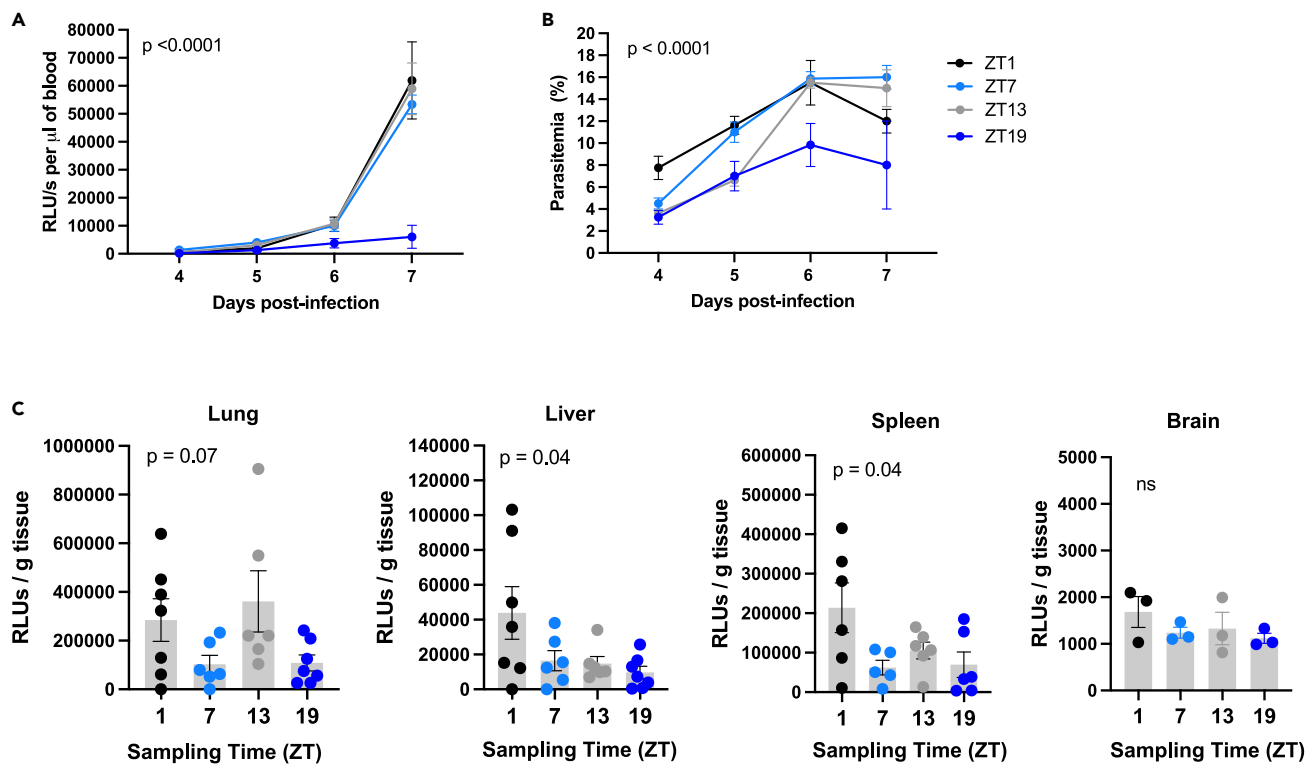


Figure 3. Parasite growth is affected by the time of infection

Mice were injected with *Plasmodium berghei* ANKA-infected erythrocytes at ZT1, 7, 13, or 19.

(A) Parasite load in the blood of infected mice, across the days of infection, measured by bioluminescence.

(B) Percentage of infected erythrocytes (parasitemia) across the days of infection.

(C) Parasite load in the brain and in three peripheral organs measured upon sacrifice (day 7 post-infection), by bioluminescence.

Data are from one of three independent experiments performed, all with similar results, with 8–11 mice per group in each. Data are shown as mean \pm SEM. Two-way ANOVA (A, B); one-way ANOVA with Tukey's multiple comparisons test (C). See also [Figures S1, S3, and S4](#).

sample). Both blood parasite load ([Figure 3A](#)) and parasitemia ([Figure 3B](#)) were affected, with lowest levels in mice infected at ZT19, with a larger time-dependent difference for parasite load. To address this apparent difference between the two measures, we extended the parasitemia data by measuring the numbers of parasites per iRBC. We noticed a reduced presence of multi-infected cells in ZT19-infected mice ([Figure S1B](#)), which might explain why the effect of time appears stronger for parasite load. Consistent with the blood data ([Figure 3A](#)), parasite load in peripheral organs such as the lung, liver, and spleen ([Figure 3C](#)) also showed decreased levels in mice infected at ZT19. Brain parasite load was very low ([Figure 3C](#)), as expected given that in the ECM model, *P. berghei* ANKA parasites are not sequestered in the brain.³⁶

Since a rhythmic pattern in hematopoietic stem and progenitor cells has been observed,³⁷ we then hypothesized that rhythms in erythrocyte (RBC) abundance could underlie parasite invasion efficacy and the establishment of the infection. Blood and spleen were collected at ZT7 or ZT19 and cells were stained for different populations of erythrocytes (gating strategy in [Figure S2](#)). Although the total population of erythrocytes (CD45⁺, Ter119⁺ cells) was not different between time points in the blood ([Figure S3A](#)), both early and late reticulocyte subsets were lower in ZT19-infected mice. Additionally, early reticulocytes were also reduced in uninfected control mice sampled at ZT19 ([Figure 4A](#)). In the spleen, there was a decrease in total erythrocytes at sampling time ZT19, counterbalanced by an increased frequency of immune cells ([Figure S3A](#)) and a reduced frequency of early reticulocytes in the controls ([Figure 4A](#)).

To determine if the time-dependent variation in erythrocyte subsets led to differences in the efficacy of parasite invasion, we looked at the proportion of cells with internalized parasites (GFP⁺) ([Figures 4B, 4C, and S3B](#)). In accordance with our parasitemia and parasite load data, ZT19-infected mice showed a lower frequency of infected erythrocytes in the blood and spleen ([Figure 4B](#)). However, among the erythrocyte subsets, only infected normocytes in the blood were decreased in ZT19-infected mice, whereas infected late reticulocytes were increased in the spleen ([Figure 4C](#)). As the spleen has been shown to be a more parasitism target,³⁸ we compared the frequency of infected erythrocytes in both compartments and detected an increased accumulation of infected cells in the spleen on day 4 post-infection ([Figure S3B](#)). We have also confirmed the preference for parasite invasion of immature erythrocytes as opposed to mature cells (normocytes) ([Figure S3B](#)).

In summary, we showed that the time of infection affects parasite growth, with impairments in ZT19-infected mice. Furthermore, our data suggest that a time-of-day variation in erythrocytes and their subsets contributes to parasite invasion efficacy.

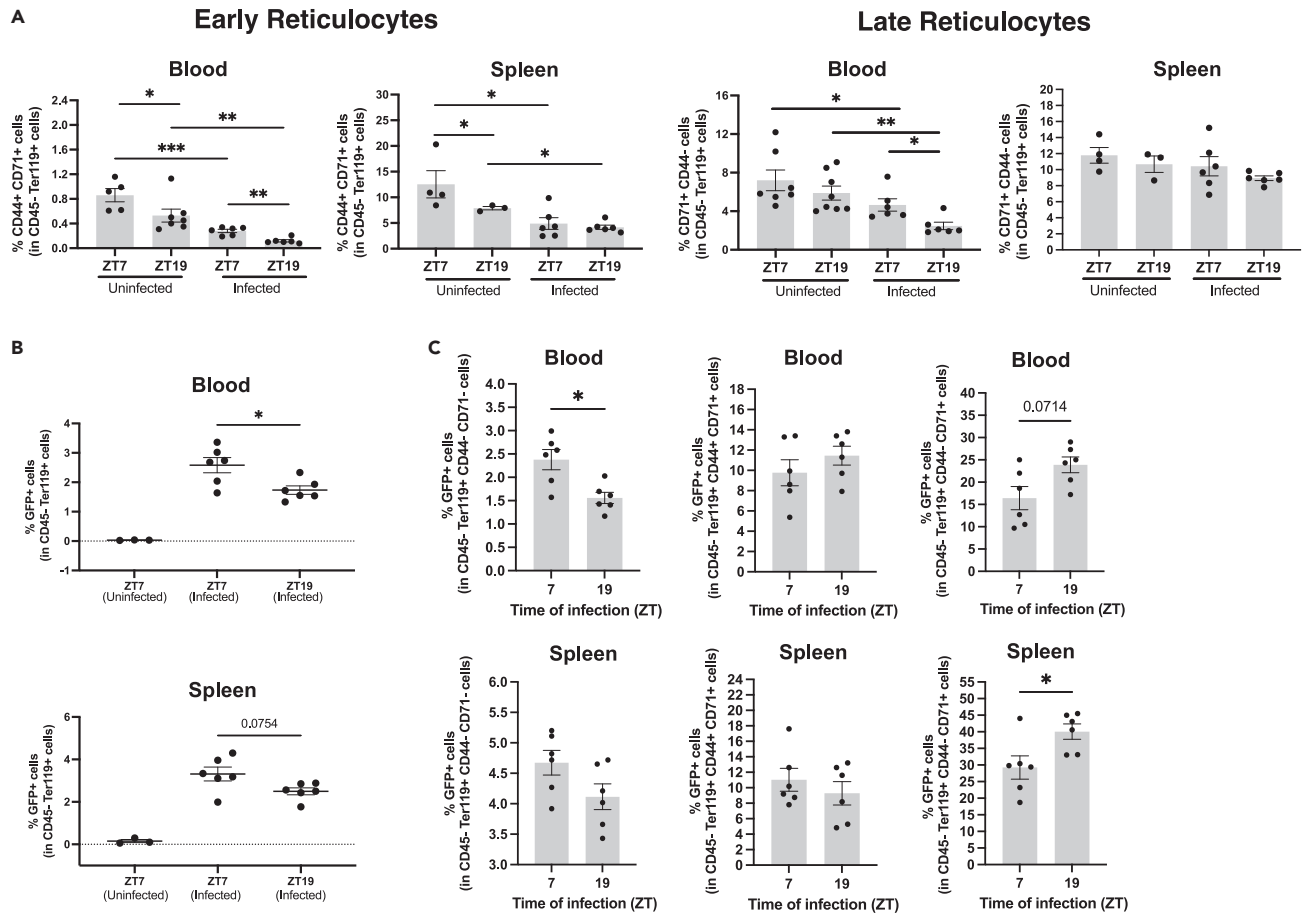


Figure 4. ZT19-infected mice have fewer infected cells

(A) Frequency of early reticulocytes (CD44⁺ CD71⁺ cells [in CD45⁻ Ter119⁺ cells]) and late reticulocytes (CD44⁻ CD71⁺ cells [in CD45⁻ Ter119⁺ cells]) in the blood and spleen of uninfected mice sampled at ZT7 or ZT19 (left), and of mice infected at ZT7 and sampled at ZT7, or infected at ZT19 and sampled at ZT19. (B) Frequency of infected erythrocytes (GFP⁺ cells [in CD45⁻ Ter119⁺ cells]) in the blood and spleen of mice infected at ZT7 or ZT19. (C) Frequency of infected normocytes (GFP⁺ cells [in CD45⁻ Ter119⁺ CD44⁻ CD71⁻ cells]), infected early reticulocytes (GFP⁺ cells [in CD45⁻ Ter119⁺ CD44⁺ CD71⁺ cells]), and infected late reticulocytes (GFP⁺ cells [in CD45⁻ Ter119⁺ CD44⁻ CD71⁺ cells]).

Data are from one of two independent experiments performed, with similar results, containing 3–8 mice per group in each. Data are shown as mean \pm SEM. One-way ANOVA with Tukey's multiple comparisons test (A, B), or Mann-Whitney test (C). * $p < 0.05$, ** $p < 0.01$, *** $p < 0.001$. See also Figures S2 and S3.

The clock transcription factor REV-ERB α is important for the high parasite load following infection in the daytime

Many aspects of the immune system are regulated by the circadian clock.^{39,40} REV-ERB α is a clock transcription factor with a rhythmic expression, which is known to rhythmically regulate the expression of many clock-controlled genes. In particular, it was shown that REV-ERB α controls inflammatory pathways in innate immune cells, e.g., cytokine/chemokine production.^{41–43} We found that infection in the daytime (ZT7) of *Rev-erb α* knockout mice (which are not arrhythmic but present defects in some immune circadian rhythms) led to a reduced parasite load compared to wild-type littermates, with unchanged values for parasitemia and host response, including survival (Figure S4). These results suggest that the higher parasite load in mice infected in the daytime is promoted by the activity of the host clock factor REV-ERB α .

Long-term circadian disruption affects parasite growth

We next investigated the effects of a chronic systemic desynchronization of host circadian clocks on ECM. Mice were subjected to a “weekly jet lag protocol” (6-h weekly phase advance of light-dark [LD] cycle, over 4 weeks) before infection with *P. berghei* ANKA iRBCs and kept under this protocol throughout the infection. This jet lag protocol did not lead to changes in host response or parasite progression, in comparison to a control 12:12 LD group (Figure S5).

We then used a more disruptive approach with an 8-h phase advance every 2 days for a total of 10 weeks. Using this long-term circadian disruption protocol, mouse survival (Figure S6A) or development of ECM (Figure S6B) were not affected. Of note though, the behavioral score of mice under the jet lag procedure showed a trend toward a delayed development of the disease (ANOVA main effect of condition,

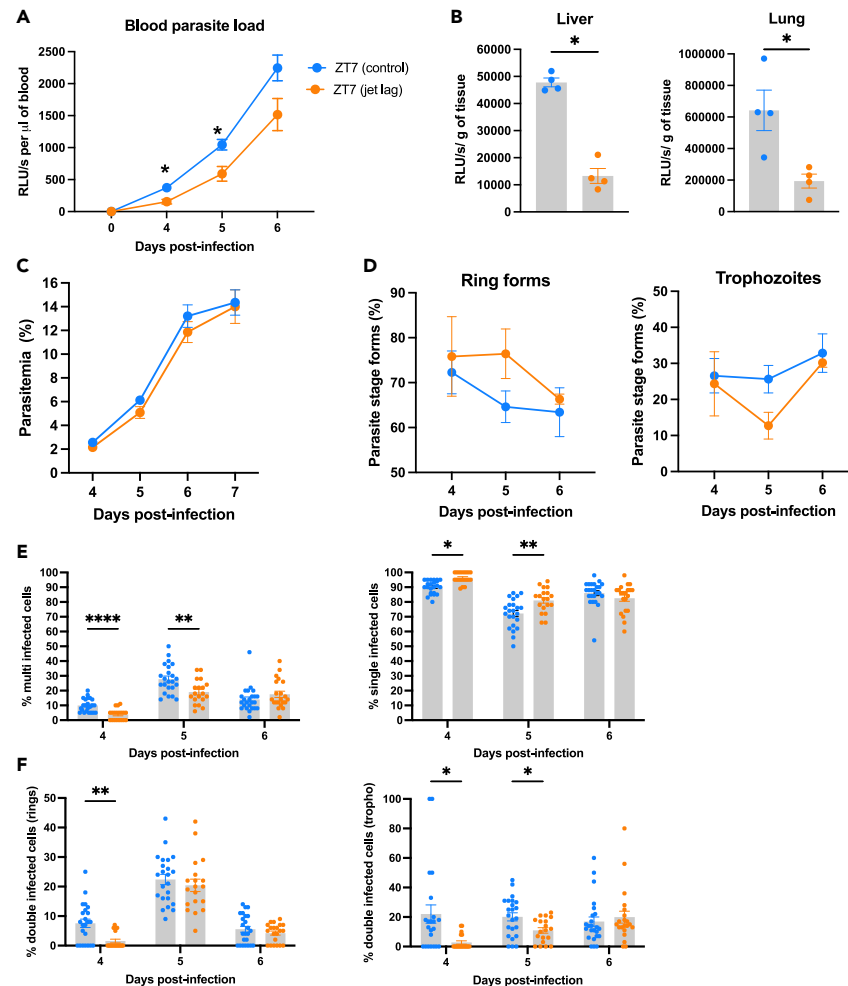


Figure 5. Circadian disruption affects parasite growth and number of parasites per cell

Mice were infected at ZT7 after the 10-week chronic jet lag protocol (jet lag) or regular 12:12 LD cycle (control).

(A and B) Parasite load in the blood (A) or in peripheral organs (B) of infected mice, across days of infection, measured by bioluminescence.

(C–F) Percentage of infected erythrocytes (parasitemia) (C), infected erythrocytes containing ring stage forms or trophozoites (D), single-infected and multi-infected erythrocytes (E), and double-infected cells with trophozoites or ring stage forms (F), across days of infections. Data are from one of three independent experiments performed, all with similar results, containing 8–10 mice per group in each, and a sum of three independent experiments for (E) and (F), containing 8–10 mice per group.

Data are shown as mean \pm SEM. Mixed-effects model (REML) with Sidak multiple comparisons test; and one-way ANOVA with Tukey's multiple comparisons test; and Mann-Whitney test. * $p < 0.05$, ** $p < 0.01$, **** $p < 0.0001$. See also [Figures S5–S7](#).

$p = 0.0927$). T cell activation, as measured in the spleen of infected mice, is a reliable predictor of ECM progression.⁴⁴ In accordance with the neurological symptoms ([Figure S6B](#)), the frequency of activated CD8⁺ T cells in the spleen was not affected by the jet lag procedure ([Figures S6C and S6D](#)). On the other hand, large effects were seen with respect to parasite growth: “jet lag” mice showed a reduced parasite load in the blood, lung, and liver ([Figures 5A and 5B](#)).

As a reduced parasite load was also an outcome observed when mice were infected at ZT19 vs. ZT7 ([Figures 3A and 3C](#)), we ran another cohort with 3 experimental groups (a ZT7, a ZT19, and a “jet lag” group infected at ZT7). As expected, both the ZT19-infected mice and the jet lag mice had a reduced parasite load compared to ZT7-infected mice ([Figure S6E](#)).

Long-term circadian disruption also affects parasite growth in *P. chabaudi*

To test whether the effect of circadian disruption on parasite growth is specific to *P. berghei* ANKA or rather applies to other *Plasmodium* species, including those whose intraerythrocytic development cycle (IDC) is synchronized, we infected mice with *P. chabaudi*, after 10 weeks of the jet lag procedure, or a control light-dark cycle. Since *P. chabaudi* IDC is synchronized in iRBCs, blood was sampled twice a day, between days 6 and 8 post-infection ([Figure S7](#)). As expected,^{22,45} the frequency of trophozoites was higher in RBCs of blood sampled in the night

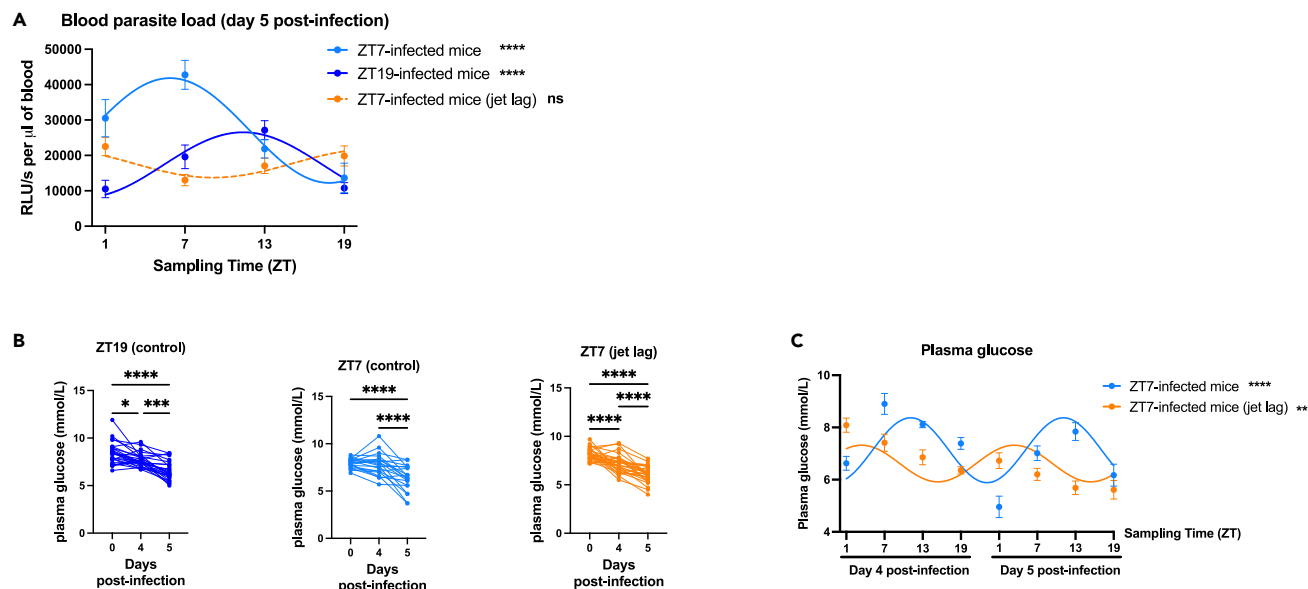


Figure 6. Rhythms in blood parasite load and plasma glucose are disrupted in jet lag mice

Mice were infected at ZT7 after 10 weeks of chronic jet lag (jet lag), or at ZT7 or ZT19 after 10 weeks of regular 12:12 LD cycle (control).

(A) Rhythms in blood parasite load of infected mice, every 6 h on day 5 post-infection, measured by bioluminescence.

(B) Levels of plasma glucose over days of infection.

(C) Rhythms in plasma glucose on days 4 and 5 post-infection.

Data are from one of three independent experiments performed, all with similar results, with 8–10 mice per group in each. Data are shown as mean \pm SEM. Rhythmicity (A, C) was evaluated by non-linear regression (cosine curve-fit) (dashed lines represent a lack of statistical significance), or one-way ANOVA with Tukey's multiple comparisons test (B). * $p < 0.05$, ** $p < 0.01$, *** $p < 0.001$, **** $p < 0.0001$. ns = not significant. See also [Figures S6](#) and [S8](#).

(ZT14) compared to the day (ZT2). Importantly, the time-dependent difference in trophozoites was not simply due to parasite synchronization, as parasitemia on day 8 post-infection revealed a similar significant difference between ZT2 and ZT14 in the control mice ([Figure S7C](#)). In contrast, such a day-night difference was blunted in mice of the jet lag group, with reduced parasitemia levels in the early night.

Long-term circadian disruption affects the frequency of multi-infected RBCs

Of interest, the reduction of parasite load (which measures total amount of parasite in the blood or tissue) upon infection with *P. berghei* ANKA under a jet lag protocol was not associated with changes in parasitemia levels (i.e., percentage of infected RBCs) and parasite stage forms ([Figures 5C](#) and [5D](#)). Therefore, given the known ability of *Plasmodium* spp. to poly-parasitize erythrocytes,⁴⁶ we re-analyzed the blood smears to assess to the number of parasites per RBC. Consistent with the blood load data, jet lag mice had fewer multi-infected cells and more single infected cells on days 4 and 5 post-infection ([Figure 5E](#)). Among these cells, there were significantly fewer RBCs infected with 2 parasites per cell in the jet lag group compared to controls (for both cells infected with either trophozoites or ring stage forms) ([Figure 5F](#)). Altogether, these data show that the reduced parasite load induced by circadian disruption is associated with a reduced parasite/RBC ratio. This could account for the reduction of parasite load without a parallel change in parasitemia.

Rhythms in blood parasite load are absent in jet lag mice

We next investigated whether blood parasite load follows a 24-h rhythm over the course of the infection. For this purpose, mice were infected as previously described (at ZT7 or ZT19 under 12:12 LD or ZT7 under jet lag) and blood was collected every 6 h on day 5 post-infection, generating 4 sampling time points (ZT1, 7, 13, and 19) ([Figure S8A](#)). For each mouse, there was a significant rhythm for ZT7- ($p < 0.0001$) and ZT19-infected mice ($p < 0.001$), with an acrophase between ZT7 and ZT13. Interestingly, rhythmicity was lost in jet lag mice, with similar and low levels at all sampling time points ([Figure 6A](#)). Parasitemia data for each stage form suggest that the variation over the day in parasite load is not due to a daily rhythm in parasite intraerythrocytic cycle ([Figure S8B](#)).

Plasma glucose is altered in jet lag mice

Since glucose was shown to induce parasite growth (schizogony) in *P. chabaudi*,²² we quantified glucose in plasma from mice sampled every 6 h on days 4 and 5 post-infection. As expected for *P. berghei* ANKA infection, mice of all groups (ZT7, ZT19, and jet lag) developed hypoglycemia throughout the infection⁴⁷ ([Figures 6B](#) and [S8C](#)). A robust rhythm of glucose was observed for control mice whereas jet lag mice had

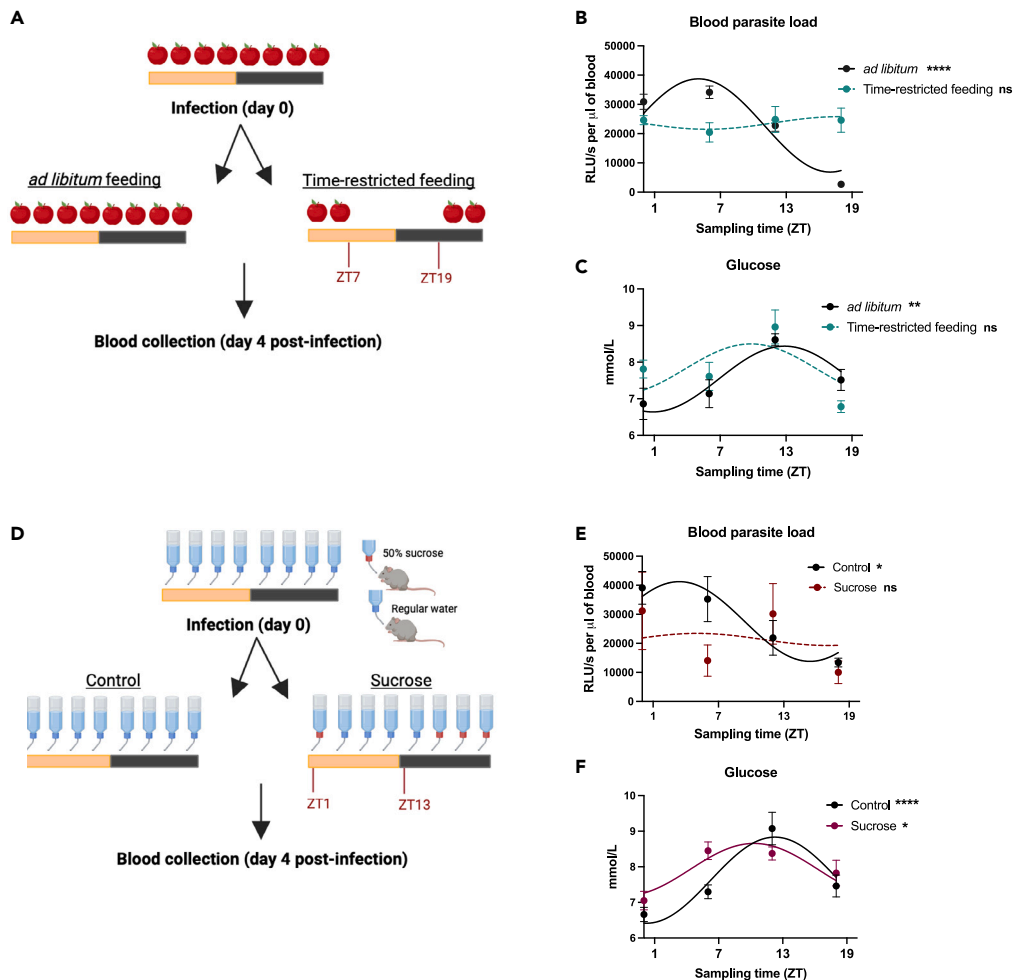


Figure 7. Rhythms in blood glucose and parasite load are disrupted following time-restricted feeding and sucrose administration in infected mice

Mice were infected and subjected to either time-restricted feeding or sucrose administration.

(A) 24 h after infection, mice were allocated to either a “time-restricted feeding” group, with access to food only between ZT19 and ZT7 or to an “ad libitum” group, with food available *ad libitum*. Mice were subjected to the protocol daily until day 4 post-infection, when blood was collected every 6 h.

(B and C) Levels of blood parasite load (B) and plasma glucose (C).

(D) 24 h after infection, mice were allocated to either a “sucrose” group, with access to 50% sucrose water only between ZT13 and ZT1, or to an “ad libitum” group, with water available *ad libitum*. Mice were subjected to the protocol daily until day 4 post-infection, when blood was collected every 6 h.

(E and F) Levels of blood parasite load (E) and plasma glucose (F).

Data are from one of two independent experiments performed, with similar results, with 8 mice per group in each. Data are shown as mean \pm SEM. Rhythmicity (B, C, E, F) was evaluated by non-linear regression (cosine curve-fit) (dashed lines represent a lack of statistical significance). * $p < 0.05$, ** $p < 0.01$, **** $p < 0.0001$. ns = not significant. Illustrations (A, D) were created with BioRender.com.

a rhythm with a sharp decreased amplitude and a phase-advance (Figure 6C). Taken together, the loss of rhythm in blood parasite load upon circadian disruption is paralleled by a greatly reduced rhythmicity of plasma glucose during *P. berghei* ANKA infection.

Parasite load rhythmicity is affected by time-restricted feeding and high sucrose administration

The concurrent effects of the jet lag protocol on parasite load and glucose rhythms suggested that host metabolism, and particularly glucose levels, might be mediating the effect of jet lag on *P. berghei* ANKA infection. To address this, we used protocols aimed at manipulating the host metabolic rhythms. First, we subjected mice to time-restricted feeding, starting after 24 h of infection until day 4 post-infection inclusively. Plasma glucose and parasite load were measured every 6 h of day 4 post-infection (Figure 7A). While control mice fed *ad libitum* group showed a rhythm of both plasma glucose and parasite load, those rhythms were abolished in mice under time-restricted feeding (Figures 7B and 7C).

Given that time-restricted feeding limits the parasite’s access to a range of food-derived nutrients, we interrogated more specifically the effect of glucose via sucrose administration: 24 h after infection, mice were given water containing 50% w/v sucrose from ZT13 to ZT1 (control

mice remained on regular water *ad libitum* (Figure 7D). Again, control mice had rhythms of glucose and parasite load, whereas in sucrose-treated mice, the parasite load rhythm was abolished and the glucose rhythm was strongly dampened (Figures 7E and 7F).

Altogether, these results indicate that host metabolism, and in particular blood glucose levels, impact parasite load rhythmicity.

DISCUSSION

In this study, we have used the ECM model in mice, involving mouse infection with *P. berghei* ANKA, to study circadian rhythms in malaria. We have focused on the phase of the disease following infected RBC rupture and activation of the immune system, and the impact on disease progression and parasite load. Indeed, the inflammatory phase of the disease as well as parasite load are key to the development of the disease in humans.⁴⁸ We reported that the growth of malaria parasite and the host response to this infection are influenced by the time of day of infection. We have also detected daily variations in the abundance of parasite's target cells (RBCs, and in particular, reticulocytes), a factor that might account for the effect of time on the course of infection. Moreover, parasite growth is also influenced by disruptive light-dark cycles. Interestingly, we showed that parasite load rhythmicity was dependent on host glucose levels. Overall, in the context of cerebral malaria, our study is the first one to look at host response and parasite growth in a time of day-dependent manner.

Initially, we showed that time of infection with *P. berghei* ANKA influences host response and the parasite's ability to establish and sustain infection in mice. We are focusing on the blood stage level of the disease. The malaria pathology in general and the cerebral malaria in particular manifest themselves at the blood stage level of the disease. Although the host does not have a control of the time of infection, the time of day at which infected RBCs are bursting and invade new cells or activate inflammatory responses is highly relevant to determine the success of infection and host symptoms/severity. A study by Deharo and colleagues⁴⁹ has looked at the parasite development cycle in RBCs after infection of mice at 13:00 and midnight (intravenously in Swiss albino mice, vs. intraperitoneally in C57BL/6 mice in our study). No changes in the IDC were observed by the authors. However, only two time points were tested (a peak of a rhythm might have been missed), and only the IDC rhythmicity was monitored. In contrast, we looked at the course of the ECM pathology, the immune response, and parasitemia and parasite load in the blood and different organs. This has allowed us to find striking differences in the course of the ECM development and in parasite load and parasitemia. Rhythms in host response are known to follow a 24 h cycle and could therefore be responsible for the observed phenotype. It was shown that the number of circulating immune cells varies across the day, with a peak during daytime (ZT4-8) in the blood of mice.⁴ Similarly, 24-h oscillations in erythrocytes were reported as a result of rhythms in progenitors' egress from bone marrow and differentiation into mature erythrocytes.³⁷ *P. berghei* ANKA has a preference for immature erythrocytes (reticulocytes) invasion,^{38,50} and an increase in reticulocyte numbers is known to enhance *P. berghei* infection,^{50,51} whereas experimentally decreasing the levels of these cells inhibits *P. berghei* development.^{52,53} Therefore, we hypothesized that rhythms in the abundance of these cells would affect the efficiency of the infection in a time-dependent manner. In line with this hypothesis, we observed a reduced frequency of both early and late reticulocytes in the blood at ZT19 compared to ZT7. Moreover, in both the blood and spleen, ZT19-infected mice had a significantly lower frequency of erythrocytes with internalized GFP⁺ parasites. The phenotype observed corroborates with the existence of migratory systemic factors, which control rhythms in cells' frequency, as shown by others in the field.^{4,5}

We have sought to determine the effects of host circadian disruption. We used a chronic jet lag approach, which was previously shown to lead to disruption of the animal's circadian rhythms.⁵⁴⁻⁵⁶ Moreover, this protocol is similar to situations of chronic circadian misalignment in humans, e.g., shift work. Night shift work in humans, and the circadian misalignment that it causes, are associated with altered immunity and metabolism.⁵⁷⁻⁶² More generally, a large part of the general population experiences disturbed rhythms due to light pollution, indoor work, or irregular schedules.^{63,64} Therefore, studying impacts of circadian disruption has relevance to the population even beyond shift workers. In rodent models, chronic circadian disruption was shown to increase the production of proinflammatory cytokines in response to lipopolysaccharide challenge,⁵⁸ to alter tumor immune microenvironment,⁶⁵ and to promote chronic inflammation in aging animals.⁵⁴ Studies with other *Plasmodium* spp. species have shown parasite dependency on environmental cues (e.g., light-dark schedules) or host circadian rhythms for parasite replication and growth.^{24,25} Thus, given the inflammatory nature of our ECM model, we originally hypothesized that circadian disruption would affect host response and parasite growth, leading to increased and faster ECM development. We used a clinical score, with multiple behavioral criteria related to the neurological pathology. While addressing the brain-related aspects of the ECM, this approach allowed us to follow the progression of the disease over time, 3 times a day, over many days. Surprisingly, we have not seen effects on these parameters, indicating that circadian disruption does not affect disease progression, development, or survival in this mouse model of cerebral malaria. A possible reason for this is a limitation of the ECM model: upon the start of the neurological phase of the disease, its progression is very fast, even though we monitored the mice 3 times per day.

Despite this, circadian disruption strongly impaired parasite growth. As reported in other *Plasmodium* spp. strains, host-parasite circadian misalignment can lead to impairments in parasite replication and generation of transmission forms (gametocytes).²⁴ In our experiments, circadian-disrupted mice consistently showed impairments in parasite load throughout the days of infection in both blood and organs (lung and liver). This reduced parasite load is relevant for the severity of the cerebral malaria disease: parasite load in peripheral tissues (and not in the brain) is associated with onset of ECM in mice,⁶⁶ and parasite load is associated with fatal outcomes in humans.⁶⁷ The reduced levels of parasite load in "jet lag" mice could be due to a reduction in the efficiency of erythrocyte invasion. In line with this, even though the frequency of infected cells (parasitemia) did not differ between the groups, the frequency of multi-infected cells on days 4 and 5 post-infection was significantly reduced in the "jet lag" mice. Multi-infected cells with either rings or trophozoites were similarly increased in "jet lag" mice, indicating that this is not restricted to a developmental stage of the parasite. This is consistent with a recent study that showed that in *P. berghei* ANKA, the proportions of each parasite stage form (ring, early and mid and late-trophozoite, and schizont) do not depend on the time of day.⁶⁸

Given the impairments on parasite growth in “jet lag” mice, we investigated if rhythms in parasite load are present during the course of ECM. *P. berghei* ANKA is known to have a partially synchronized development. Although the frequencies of each stage form of *P. berghei* ANKA are not synchronized among RBCs⁶⁸ (in contrast to e.g., *P. chabaudi*⁴⁵), the development cycle and gametocyte production exhibit a ~22 h rhythm, with a peak in the nighttime in mice.^{69,70} To ascertain that the effect of the jet lag procedure on the course of the infection was not a feature specific to *P. berghei* ANKA, jet lag experiments were also performed with the synchronous parasite *P. chabaudi*, for which we have observed a reduction in parasitemia and a blunting of the day-night difference. The lower synchronization features of *P. berghei* ANKA compared to other species can be viewed as a strength of our approach, as it allows to better isolate the effect of host rhythms on the disease and parasite load. However, it begged the question of whether rhythms of parasite load were present after infection, and if so, whether “jet lag” mice displayed altered rhythms.

Surprisingly, a rhythm in blood parasite load was detected in ZT7- and ZT19-infected mice but not in “jet lag” mice. This was paralleled by a dampening of the rhythm in plasma glucose. This would be consistent with a dependency of the parasite on host metabolism, as studies using *Plasmodium* spp. have shown that parasite proliferation requires host metabolites,^{71,72} and disruption of circadian rhythms results in altered glucose rhythms.⁷³ Moreover, host metabolism and feeding behavior regulate rhythms of *P. chabaudi* developmental cycle.^{21,22,74} To investigate this further, we assessed rhythms of plasma glucose and parasite load under time-restricted feeding. The removal of food for 12 h from ZT7 to ZT19 aimed to prevent food access during the phase when most of food consumption generally occurs.⁷⁵ Consistent with the literature, plasma glucose followed a 24-h rhythm with an acrophase at the first hours of the night.⁷⁶ We found that animals with 24-h *ad libitum* food displayed a robust rhythm of plasma glucose and parasite load, which was not observed in the time-restricted feeding mice.

When we investigated if parasite rhythms were directly modulated by host glucose, we found a similar lack of rhythm of parasite load and elevated levels of daytime plasma glucose in sucrose-administered mice, compared to control mice. Therefore, manipulating plasma glucose affects blood parasite rhythmicity. This is consistent with prior literature on the effects of host cues on rhythms of *Plasmodium* spp.,^{22,45,77–79} most of which focused on factors that impinge on the parasite IDC or regulation of parasite rhythmic gene expression. Research has shown that host glucose levels affect the progression of the IDC as well as parasite virulence.⁸⁰ Nevertheless, our observations that the parasite load does not change in the exact same way as glucose levels upon the feeding schedule or sucrose interventions suggest that additional factors besides glucose levels (e.g., other nutrients and host metabolites) contribute to the parasite rhythm, as well as other host circadian rhythms and clocks potentially affected by feeding and sucrose administration. There has been evidence for a role for isoleucine (an amino acid whose levels would be impacted by changes in feeding schedules) in regulating the IDC, making it a possible candidate molecule.⁸¹ Other work has pointed to the circadian hormone melatonin as a regulator of *Plasmodium* infection,⁷⁸ but it is unlikely to be involved in our system, as C57BL/6 mice have very low or undetectable levels of this hormone.⁸² Another important consideration is the possible implication of the parasite-intrinsic circadian rhythms, which have been uncovered in *P. chabaudi* and *P. falciparum*.^{45,83,84} However, in our experiments, the mice were infected at the same time, using the same batch of parasites, so the only factors that differ between the groups are the host cues. Moreover, mice mutant for clock gene *Rev-erb α* showed lower daytime parasite load, further emphasizing that the regulation comes from host’s circadian rhythms. The role of *Rev-erb α* in regulating inflammatory processes in innate immune cells (including cytokine production)^{41,43,85} might be one of the mechanisms underlying the effect of this knockout on the blood parasite load.

In conclusion, our study reveals novel findings demonstrating that time of infection affects host response and parasite growth *in vivo* in a mouse model of cerebral malaria and that *P. berghei* ANKA parasite load harbors a 24-h rhythm that is affected by irregular lighting conditions (chronic jet lag), time-restricted feeding, and sucrose administration. The exact nature of the host cues controlling the course of the infection remains to be determined, but our data support a model where a combination of cues would be involved, including glucose and other rhythmic or feeding-derived metabolites as well as a rhythmicity of target cells of the parasite, in particular reticulocytes. Given the known relevance of the inflammatory phase of the disease in cerebral malaria, and more generally of parasite load in malaria, our data shed light on new aspects of the disease relevant to human malaria and could contribute to new therapeutic or prophylactic measures.

Limitations of the study

Our study has some limitations. The experiments were done under light-dark conditions, rather than under constant darkness conditions, preventing to assess the endogenous (i.e., circadian) nature of the observed rhythms. Also, due to the fast-paced nature of the *P. berghei* ANKA infection model, long-term effects of time of day or circadian disruption during malaria pathogenesis could not be assessed. In determining possible mechanisms for the effect of time, in particular the parasite growth impairment in mice infected at ZT19, other host cell types could be involved, and in particular, the influence of time on the local immune response at the site of infection (peritoneal cavity) could be studied. Finally, the experiments were done only in male mice. Doing similar work in female mice would address the effect of sex on the daily regulation of experimental cerebral malaria, which would be relevant given that sex-dependent differences were found in the occurrence of malaria in humans.⁸⁶

STAR★METHODS

Detailed methods are provided in the online version of this paper and include the following:

- KEY RESOURCES TABLE
- RESOURCE AVAILABILITY
 - Lead contact

- Materials availability
- Data and code availability
- **EXPERIMENTAL MODEL AND STUDY PARTICIPANT DETAILS**
 - Mouse strains and housing conditions
 - Plasmodium spp. strains
- **METHOD DETAILS**
 - Plasmodium spp. infections
 - Time-restricted feeding protocol
 - Sucrose administration protocol
 - Mouse survival and clinical scores
 - Blood-brain barrier integrity
 - Flow cytometry
 - Parasitemia and parasite stage forms
 - Parasite load (blood and organs)
 - Cytokine/chemokine measurements
 - Glucose measurements
- **QUANTIFICATION AND STATISTICAL ANALYSIS**

SUPPLEMENTAL INFORMATION

Supplemental information can be found online at <https://doi.org/10.1016/j.isci.2024.109684>.

ACKNOWLEDGMENTS

The authors thank the members of Cermakian and Olivier laboratories for discussions, knowledge sharing, technical training, and reagents, Grace Jackson and Genavieve Maloney for proofreading of the manuscript, the Douglas Mental Health University Institute Animal Facility staff for the training and animal procedure assistance, and the Immunophenotyping Platform at the McGill University Health Care for flow cytometry assistance. This study was supported by a grant from the Canadian Institutes of Health Research (PJT-168847, to N.C. and M.O.; MOP-119322, to N.C.), and Douglas Foundation, and doctoral fellowships from Faculty of Medicine and Health Sciences - McGill (to P.C.C.) and Fonds de Recherche du Québec - Santé (to P.C.C.).

AUTHOR CONTRIBUTIONS

N.C. and M.O. received the funding for the execution of the project. P.C.C., N.C., and M.O. designed the project. P.C.C. and J.W. executed the experimental work. P.C.C. analyzed the data. P.C.C. and N.C. wrote the manuscript. All authors commented on the manuscript.

DECLARATION OF INTERESTS

The authors declare no competing interests.

Received: September 28, 2023

Revised: December 20, 2023

Accepted: April 4, 2024

Published: April 8, 2024

REFERENCES

1. Lowrey, P.L., and Takahashi, J.S. (2004). Mammalian circadian biology: elucidating genome-wide levels of temporal organization. *Annu. Rev. Genom. Hum. Genet.* 5, 407–441. <https://doi.org/10.1146/annurev.genom.5.061903.175925>.
2. Nobis, C.C., Labrecque, N., and Cermakian, N. (2018). From immune homeostasis to inflammation, a question of rhythms. *Curr. Opin. Physiol.* 5, 90–98. <https://doi.org/10.1016/j.cophys.2018.09.001>.
3. Geiger, S.S., Fagundes, C.T., and Siegel, R.M. (2015). Chrono-immunology: progress and challenges in understanding links between the circadian and immune systems. *Immunology* 146, 349–358. <https://doi.org/10.1111/imm.12525>.
4. Nguyen, K.D., Fentress, S.J., Qiu, Y., Yun, K., Cox, J.S., and Chawla, A. (2013). Circadian gene *Bmal1* regulates diurnal oscillations of *Ly6C*(hi) inflammatory monocytes. *Science* 341, 1483–1488. <https://doi.org/10.1126/science.1240636>.
5. Scheiermann, C., Kunisaki, Y., Lucas, D., Chow, A., Jang, J.E., Zhang, D., Hashimoto, D., Merad, M., and Frenette, P.S. (2012). Adrenergic nerves govern circadian leukocyte recruitment to tissues. *Immunity* 37, 290–301. <https://doi.org/10.1016/j.immuni.2012.05.021>.
6. Carvalho Cabral, P., Tekade, K., Stegeman, S.K., Olivier, M., and Cermakian, N. (2022). The involvement of host circadian clocks in the regulation of the immune response to parasitic infections in mammals. *Parasite Immunol.* 44, e12903. <https://doi.org/10.1111/pim.12903>.
7. Carvalho Cabral, P., Olivier, M., and Cermakian, N. (2019). The Complex Interplay of Parasites, Their Hosts, and Circadian Clocks. *Front. Cell. Infect. Microbiol.* 9, 425. <https://doi.org/10.3389/fcimb.2019.00425>.
8. Zhuang, X., Magri, A., Hill, M., Lai, A.G., Kumar, A., Rambhatla, S.B., Donald, C.L., Lopez-Clavijo, A.F., Rudge, S., Pinnick, K., et al. (2019). The circadian clock components *BMAL1* and *REV-ERBalpha* regulate flavivirus replication. *Nat. Commun.* 10, 377. <https://doi.org/10.1038/s41467-019-08299-7>.
9. Gibbs, J., Ince, L., Matthews, L., Mei, J., Bell, T., Yang, N., Saer, B., Begley, N., Poolman, T., Pariollaud, M., et al. (2014). An epithelial circadian clock controls pulmonary

- inflammation and glucocorticoid action. *Nat. Med.* 20, 919–926. <https://doi.org/10.1038/nm.3599>.
10. Bellet, M.M., Deriu, E., Liu, J.Z., Grimaldi, B., Blaschitz, C., Zeller, M., Edwards, R.A., Sahar, S., Dandekar, S., Baldi, P., et al. (2013). Circadian clock regulates the host response to Salmonella. *Proc. Natl. Acad. Sci. USA* 110, 9897–9902. <https://doi.org/10.1073/pnas.1120636110>.
 11. Kiessling, S., Dubeau-Laramée, G., Ohm, H., Labrecque, N., Olivier, M., and Cermakian, N. (2017). The circadian clock in immune cells controls the magnitude of Leishmania parasite infection. *Sci. Rep.* 7, 10892. <https://doi.org/10.1038/s41598-017-11297-8>.
 12. Laranjeira-Silva, M.F., Zampieri, R.A., Muxel, S.M., Floeter-Winter, L.M., and Markus, R.P. (2015). Melatonin attenuates Leishmania (L.) amazonensis infection by modulating arginine metabolism. *J. Pineal Res.* 59, 478–487. <https://doi.org/10.1111/jpi.12279>.
 13. Hopwood, T.W., Hall, S., Begley, N., Forman, R., Brown, S., Vonslow, R., Saer, B., Little, M.C., Murphy, E.A., Hurst, R.J., et al. (2018). The circadian regulator BMAL1 programmes responses to parasitic worm infection via a dendritic cell clock. *Sci. Rep.* 8, 3782. <https://doi.org/10.1038/s41598-018-22021-5>.
 14. World Health Organization (2022). *World Malaria Report 2022*. Global report.
 15. Hawking, F. (1970). The clock of the malaria parasite. *Sci. Am.* 222, 123–131. <https://doi.org/10.1038/scientificamerican0670-123>.
 16. Neva, F.A., Howard, W.A., Glew, R.H., Krotoski, W.A., Gam, A.A., Collins, W.E., Atkinson, J.P., and Frank, M.M. (1974). Relationship of serum complement levels to events of the malarial paroxysm. *J. Clin. Invest.* 54, 451–460. <https://doi.org/10.1172/JCI107781>.
 17. Mideo, N., Reece, S.E., Smith, A.L., and Metcalf, C.J.E. (2013). The Cinderella syndrome: why do malaria-infected cells burst at midnight? *Trends Parasitol.* 29, 10–16. <https://doi.org/10.1016/j.pt.2012.10.006>.
 18. Schneider, P., Rund, S.S.C., Smith, N.L., Prior, K.F., O'Donnell, A.J., and Reece, S.E. (2018). Adaptive periodicity in the infectivity of malaria gametocytes to mosquitoes. *Proc. Biol. Sci.* 285, 20181876. <https://doi.org/10.1098/rspb.2018.1876>.
 19. Rund, S.S., O'Donnell, A.J., Gentile, J.E., and Reece, S.E. (2016). Daily Rhythms in Mosquitoes and Their Consequences for Malaria Transmission. *Insects* 7, 14. <https://doi.org/10.3390/insects7020014>.
 20. Pigeault, R., Caudron, Q., Nicot, A., Rivero, A., and Gandon, S. (2018). Timing malaria transmission with mosquito fluctuations. *Evol. Lett.* 2, 378–389. <https://doi.org/10.1002/evl3.61>.
 21. Prior, K.F., van der Veen, D.R., O'Donnell, A.J., Cumnock, K., Schneider, D., Pain, A., Subudhi, A., Ramaprasad, A., Rund, S.S.C., Savill, N.J., and Reece, S.E. (2018). Timing of host feeding drives rhythms in parasite replication. *PLoS Pathog.* 14, e1006900. <https://doi.org/10.1371/journal.ppat.1006900>.
 22. Hirako, I.C., Assis, P.A., Hojo-Souza, N.S., Reed, G., Nakaya, H., Golenbock, D.T., Coimbra, R.S., and Gazzinelli, R.T. (2018). Daily Rhythms of TNF α Expression and Food Intake Regulate Synchrony of Plasmodium Stages with the Host Circadian Cycle. *Cell Host Microbe* 23, 796–808.e6. <https://doi.org/10.1016/j.chom.2018.04.016>.
 23. Rijo-Ferreira, F., Acosta-Rodriguez, V.A., Abel, J.H., Kornblum, I., Bento, I., Kilaru, G., Klerman, E.B., Mota, M.M., and Takahashi, J.S. (2020). Malaria has an intrinsic clock. *Science* 368, 746–753. <https://doi.org/10.1126/science.aba2658>.
 24. O'Donnell, A.J., Schneider, P., McWatters, H.G., and Reece, S.E. (2011). Fitness costs of disrupting circadian rhythms in malaria parasites. *Proc. Biol. Sci.* 278, 2429–2436. <https://doi.org/10.1098/rspb.2010.2457>.
 25. O'Donnell, A.J., Mideo, N., and Reece, S.E. (2013). Disrupting rhythms in Plasmodium chabaudii: costs accrue quickly and independently of how infections are initiated. *Malar. J.* 12, 372. <https://doi.org/10.1186/1475-2875-12-372>.
 26. Dunst, J., Kamena, F., and Matuschewski, K. (2017). Cytokines and Chemokines in Cerebral Malaria Pathogenesis. *Front. Cell. Infect. Microbiol.* 7, 324. <https://doi.org/10.3389/fcimb.2017.00324>.
 27. Lou, J., Lucas, R., and Grau, G.E. (2001). Pathogenesis of cerebral malaria: recent experimental data and possible applications for humans. *Clin. Microbiol. Rev.* 14, 810–820. <https://doi.org/10.1128/CMR.14.4.810-820.2001>.
 28. White, N.J., Turner, G.D.H., Medana, I.M., Dondorp, A.M., and Day, N.P.J. (2010). The murine cerebral malaria phenomenon. *Trends Parasitol.* 26, 11–15. <https://doi.org/10.1016/j.pt.2009.10.007>.
 29. Ghazanfari, N., Mueller, S.N., and Heath, W.R. (2018). Cerebral Malaria in Mouse and Man. *Front. Immunol.* 9, 2016. <https://doi.org/10.3389/fimmu.2018.02016>.
 30. Howland, S.W., Poh, C.M., Gun, S.Y., Claser, C., Malleret, B., Shastri, N., Ginhoux, F., Grotenbreg, G.M., and Rénia, L. (2013). Brain microvessel cross-presentation is a hallmark of experimental cerebral malaria. *EMBO Mol. Med.* 5, 984–999. <https://doi.org/10.1002/emmm.201202273>.
 31. Kassa, F.A., Van Den Ham, K., Rainone, A., Fournier, S., Boilard, E., and Olivier, M. (2016). Absence of apolipoprotein E protects mice from cerebral malaria. *Sci. Rep.* 6, 33615. <https://doi.org/10.1038/srep33615>.
 32. Akkaya, M., Bansal, A., Sheehan, P.W., Pena, M., Cimperman, C.K., Qi, C.F., Yazew, T., Otto, T.D., Billker, O., Miller, L.H., and Pierce, S.K. (2020). Testing the impact of a single nucleotide polymorphism in a Plasmodium berghei ApiAP2 transcription factor on experimental cerebral malaria in mice. *Sci. Rep.* 10, 13630. <https://doi.org/10.1038/s41598-020-70617-7>.
 33. Dobbs, K.R., Crabtree, J.N., and Dent, A.E. (2020). Innate immunity to malaria—The role of monocytes. *Immunol. Rev.* 293, 8–24. <https://doi.org/10.1111/imr.12830>.
 34. Shio, M.T., Kassa, F.A., Bellemare, M.J., and Olivier, M. (2010). Innate inflammatory response to the malarial pigment hemozoin. *Microb. Infect.* 12, 889–899. <https://doi.org/10.1016/j.micinf.2010.07.001>.
 35. Gazzinelli, R.T., Kalantari, P., Fitzgerald, K.A., and Golenbock, D.T. (2014). Innate sensing of malaria parasites. *Nat. Rev. Immunol.* 14, 744–757. <https://doi.org/10.1038/nri3742>.
 36. Franke-Fayard, B., Fonager, J., Braks, A., Khan, S.M., and Janse, C.J. (2010). Sequestration and tissue accumulation of human malaria parasites: can we learn anything from rodent models of malaria? *PLoS Pathog.* 6, e1001032. <https://doi.org/10.1371/journal.ppat.1001032>.
 37. Golan, K., Kumari, A., Kollet, O., Khatib-Massalha, E., Subramaniam, M.D., Ferreira, Z.S., Avemaria, F., Rzeszotek, S., Garcia-García, A., Xie, S., et al. (2018). Daily Onset of Light and Darkness Differentially Controls Hematopoietic Stem Cell Differentiation and Maintenance. *Cell Stem Cell* 23, 572–585.e7. <https://doi.org/10.1016/j.stem.2018.08.002>.
 38. Hentzschel, F., Gibbins, M.P., Attipa, C., Beraldi, D., Moxon, C.A., Otto, T.D., and Marti, M. (2022). Host cell maturation modulates parasite invasion and sexual differentiation in Plasmodium berghei. *Sci. Adv.* 8, eabm7348. <https://doi.org/10.1126/sciadv.abm7348>.
 39. Labrecque, N., and Cermakian, N. (2015). Circadian Clocks in the Immune System. *J. Biol. Rhythm.* 30, 277–290. <https://doi.org/10.1177/0748730415577723>.
 40. Wang, C., Lutes, L.K., Barnoud, C., and Scheiermann, C. (2022). The circadian immune system. *Sci. Immunol.* 7, eabm2465. <https://doi.org/10.1126/sciimmunol.abm2465>.
 41. Gibbs, J.E., Blaikley, J., Beesley, S., Matthews, L., Simpson, K.D., Boyce, S.H., Farrow, S.N., Else, K.J., Singh, D., Ray, D.W., and Loudon, A.S.I. (2012). The nuclear receptor REV-ERB α mediates circadian regulation of innate immunity through selective regulation of inflammatory cytokines. *Proc. Natl. Acad. Sci. USA* 109, 582–587. <https://doi.org/10.1073/pnas.1106750109>.
 42. Sato, S., Sakurai, T., Ogasawara, J., Takahashi, M., Izawa, T., Imaizumi, K., Taniguchi, N., Ohno, H., and Kizaki, T. (2014). A circadian clock gene, Rev-erb α , modulates the inflammatory function of macrophages through the negative regulation of Ccl2 expression. *J. Immunol.* 192, 407–417. <https://doi.org/10.4049/jimmunol.1301982>.
 43. Pariollaud, M., Gibbs, J.E., Hopwood, T.W., Brown, S., Begley, N., Vonslow, R., Poolman, T., Guo, B., Saer, B., Jones, D.H., et al. (2018). Circadian clock component REV-ERB α controls homeostatic regulation of pulmonary inflammation. *J. Clin. Invest.* 128, 2281–2296. <https://doi.org/10.1172/JCI93910>.
 44. Freire-Antunes, L., Ornellas-García, U., Rangel-Ferreira, M.V., Ribeiro-Almeida, M.L., de Sousa, C.H.G., Carvalho, L.J.D.M., Daniel-Ribeiro, C.T., and Ribeiro-Gomes, F.L. (2023). Increased Neutrophil Percentage and Neutrophil-T Cell Ratio Precedes Clinical Onset of Experimental Cerebral Malaria. *Int. J. Mol. Sci.* 24, 11332. <https://doi.org/10.3390/ijms241411332>.
 45. Rijo-Ferreira, F., Acosta-Rodriguez, V.A., Abel, J.H., Kornblum, I., Bento, I., Kilaru, G., Klerman, E.B., Mota, M.M., and Takahashi, J.S. (2020). The malaria parasite has an intrinsic clock. *Science* 368, 746–753. <https://doi.org/10.1126/science.aba2658>.
 46. Chotivanich, K., Udomsangpetch, R., Simpson, J.A., Newton, P., Pukrittayakamee, S., Looareesuwan, S., and White, N.J. (2000). Parasite multiplication potential and the severity of Falciparum malaria. *J. Infect. Dis.* 181, 1206–1209. <https://doi.org/10.1086/315353>.
 47. Ounjaijean, S., Chachiyo, S., and Somsak, V. (2019). Hypoglycemia induced by Plasmodium berghei infection is prevented by treatment with Tinospira crispa stem extract. *Parasitol. Int.* 68, 57–59. <https://doi.org/10.1016/j.parint.2018.10.009>.

48. Coban, C., Lee, M.S.J., and Ishii, K.J. (2018). Tissue-specific immunopathology during malaria infection. *Nat. Rev. Immunol.* **18**, 266–278. <https://doi.org/10.1038/nri.2017.138>.
49. Deharo, E., Coquelin, F., Chabaud, A.G., and Landau, I. (1996). The erythrocytic schizogony of two synchronized strains of *Plasmodium berghei*, NK65 and ANKA, in normocytes and reticulocytes. *Parasitol. Res.* **82**, 178–182. <https://doi.org/10.1007/s004360050091>.
50. Schwink, T.M. (1960). The effect of anti-erythrocytic antibodies upon *Plasmodium berghei* infections in white mice. *Am. J. Trop. Med. Hyg.* **9**, 293–296. <https://doi.org/10.4269/ajtmh.1960.9.293>.
51. Ott, K.J. (1968). Influence of reticulocytosis on the course of infection of *Plasmodium chabaudi* and *P. berghei*. *J. Protozool.* **15**, 365–369. <https://doi.org/10.1111/j.1550-7408.1968.tb02138.x>.
52. Cox, F.E. (1974). A comparative account of the effects of betamethasone on mice infected with *Plasmodium vinckei chabaudi* and *Plasmodium berghei yoelii*. *Parasitology* **68**, 19–26. <https://doi.org/10.1017/s0031182000045339>.
53. Ladda, R.L. (1966). Morphologic observations on the effect of antimalarial agents on the erythrocytic forms of *Plasmodium berghei* *in vitro*. *Mil. Med.* **131** (Suppl), 993–1008.
54. Inokawa, H., Umemura, Y., Shimba, A., Kawakami, E., Koike, N., Tsuchiya, Y., Ohashi, M., Minami, Y., Cui, G., Asahi, T., et al. (2020). Chronic circadian misalignment accelerates immune senescence and abbreviates lifespan in mice. *Sci. Rep.* **10**, 2569. <https://doi.org/10.1038/s41598-020-59541-y>.
55. Casiraghi, L.P., Oda, G.A., Chiesa, J.J., Friesen, W.O., and Golombek, D.A. (2012). Forced desynchronization of activity rhythms in a model of chronic jet lag in mice. *J. Biol. Rhythm.* **27**, 59–69. <https://doi.org/10.1177/0748730411429447>.
56. Castanon-Cervantes, O., Wu, M., Ehlen, J.C., Paul, K., Gamble, K.L., Johnson, R.L., Besing, R.C., Menaker, M., Gewirtz, A.T., and Davidson, A.J. (2010). Dysregulation of inflammatory responses by chronic circadian disruption. *J. Immunol.* **185**, 5796–5805. <https://doi.org/10.4049/jimmunol.1001026>.
57. Cuesta, M., Boudreau, P., Dubeau-Laramée, G., Cermakian, N., and Boivin, D.B. (2016). Simulated Night Shift Disrupts Circadian Rhythms of Immune Functions in Humans. *J. Immunol.* **196**, 2466–2475. <https://doi.org/10.4049/jimmunol.1502422>.
58. Kervezee, L., Cuesta, M., Cermakian, N., and Boivin, D.B. (2018). Simulated night shift work induces circadian misalignment of the human peripheral blood mononuclear cell transcriptome. *Proc. Natl. Acad. Sci. USA* **115**, 5540–5545. <https://doi.org/10.1073/pnas.1720719115>.
59. Kervezee, L., Koshy, A., Cermakian, N., and Boivin, D.B. (2023). The Effect of Night Shifts on 24-h Rhythms in the Urinary Metabolome of Police Officers on a Rotating Work Schedule. *J. Biol. Rhythm.* **38**, 64–76. <https://doi.org/10.1177/07487304221132088>.
60. Butler, T., Maidstone, J.R., Rutter, K.M., McLaughlin, T.J., Ray, W.D., and Gibbs, E.J. (2023). The Associations of Chronotype and Shift Work With Rheumatoid Arthritis. *J. Biol. Rhythm.* **38**, 510–518. <https://doi.org/10.1177/07487304231179595>.
61. Morris, C.J., Purvis, T.E., Mistretta, J., and Scheer, F.A.J.L. (2016). Effects of the Internal Circadian System and Circadian Misalignment on Glucose Tolerance in Chronic Shift Workers. *J. Clin. Endocrinol. Metab.* **101**, 1066–1074. <https://doi.org/10.1210/jc.2015-3924>.
62. Kervezee, L., Kosmadopoulos, A., and Boivin, D.B. (2020). Metabolic and cardiovascular consequences of shift work: The role of circadian disruption and sleep disturbances. *Eur. J. Neurosci.* **51**, 396–412. <https://doi.org/10.1111/ejn.14216>.
63. Fishbein, A.B., Knutson, K.L., and Zee, P.C. (2021). Circadian disruption and human health. *J. Clin. Invest.* **131**, e148286. <https://doi.org/10.1172/JCI148286>.
64. Zielinska-Dabkowska, K.M., Schernhammer, E.S., Hanifin, J.P., and Brainard, G.C. (2023). Reducing nighttime light exposure in the urban environment to benefit human health and society. *Science* **380**, 1130–1135. <https://doi.org/10.1126/science.adg5277>.
65. Aiello, I., Fedele, M.L.M., Román, F., Marpegan, L., Caldart, C., Chiesa, J.J., Golombek, D.A., Finkielstein, C.V., and Paladino, N. (2020). Circadian disruption promotes tumor-immune microenvironment remodeling favoring tumor cell proliferation. *Sci. Adv.* **6**, eaaz4530. <https://doi.org/10.1126/sciadv.aaz4530>.
66. Amante, F.H., Haque, A., Stanley, A.C., Rivera, F.d.L., Randall, L.M., Wilson, Y.A., Yeo, G., Pieper, C., Crabb, B.S., de Koning-Ward, T.F., et al. (2010). Immune-mediated mechanisms of parasite tissue sequestration during experimental cerebral malaria. *J. Immunol.* **185**, 3632–3642. <https://doi.org/10.4049/jimmunol.1000944>.
67. Pongponratn, E., Turner, G.D.H., Day, N.P.J., Phu, N.H., Simpson, J.A., Stepniowska, K., Mai, N.T.H., Viriyavejikul, P., Looareesuwan, S., Hien, T.T., et al. (2003). An ultrastructural study of the brain in fatal *Plasmodium falciparum* malaria. *Am. J. Trop. Med. Hyg.* **69**, 345–359.
68. O'Donnell, A.J., and Reece, S.E. (2021). Ecology of asynchronous asexual replication: the intraerythrocytic development cycle of *Plasmodium berghei* is resistant to host rhythms. *Malar. J.* **20**, 105. <https://doi.org/10.1186/s12936-021-03643-z>.
69. Orbán, Á., Rebelo, M., Molnár, P., Albuquerque, I.S., Butykai, A., and Kézsmárki, I. (2016). Efficient monitoring of the blood-stage infection in a malaria rodent model by the rotating-crystal magneto-optical method. *Sci. Rep.* **6**, 23218. <https://doi.org/10.1038/srep23218>.
70. Khoury, D.S., Cromer, D., Akter, J., Sebina, I., Elliott, T., Thomas, B.S., Soon, M.S.F., James, K.R., Best, S.E., Haque, A., and Davenport, M.P. (2017). Host-mediated impairment of parasite maturation during blood-stage *Plasmodium* infection. *Proc. Natl. Acad. Sci. USA* **114**, 7701–7706. <https://doi.org/10.1073/pnas.1618939114>.
71. Gordon, E.B., Hart, G.T., Tran, T.M., Waisberg, M., Akkaya, M., Kim, A.S., Hamilton, S.E., Pena, M., Yazew, T., Qi, C.F., et al. (2015). Targeting glutamine metabolism rescues mice from late-stage cerebral malaria. *Proc. Natl. Acad. Sci. USA* **112**, 13075–13080. <https://doi.org/10.1073/pnas.1516544112>.
72. Ke, H., Lewis, I.A., Morrisey, J.M., McLean, K.J., Ganesan, S.M., Painter, H.J., Mather, M.W., Jacobs-Lorena, M., Llinás, M., and Vaidya, A.B. (2015). Genetic investigation of tricarboxylic acid metabolism during the *Plasmodium falciparum* life cycle. *Cell Rep.* **11**, 164–174. <https://doi.org/10.1016/j.celrep.2015.03.011>.
73. la Fleur, S.E., Kalsbeek, A., Wortel, J., Fekkes, M.L., and Buijs, R.M. (2001). A daily rhythm in glucose tolerance: a role for the suprachiasmatic nucleus. *Diabetes* **50**, 1237–1243. <https://doi.org/10.2337/diabetes.50.6.1237>.
74. O'Donnell, A.J., Greischar, M.A., and Reece, S.E. (2022). Mistimed malaria parasites re-synchronize with host feeding-fasting rhythms by shortening the duration of intra-erythrocytic development. *Parasite Immunol.* **44**, e12898. <https://doi.org/10.1111/pim.12898>.
75. Bowe, J.E., Franklin, Z.J., Hauge-Evans, A.C., King, A.J., Persaud, S.J., and Jones, P.M. (2014). Metabolic phenotyping guidelines: assessing glucose homeostasis in rodent models. *J. Endocrinol.* **222**, G13–G25. <https://doi.org/10.1530/JOE-14-0182>.
76. Jensen, T.L., Kiersgaard, M.K., Sørensen, D.B., and Mikkelsen, L.F. (2013). Fasting of mice: a review. *Lab. Anim.* **47**, 225–240. <https://doi.org/10.1177/0023677213501659>.
77. Motta, F.C., McGoff, K., Moseley, R.C., Cho, C.Y., Kelliher, C.M., Smith, L.M., Ortiz, M.S., Leman, A.R., Campione, S.A., Devos, N., et al. (2023). The parasite intraerythrocytic cycle and human circadian cycle are coupled during malaria infection. *Proc. Natl. Acad. Sci. USA* **120**, e2216522120. <https://doi.org/10.1073/pnas.2216522120>.
78. Hotta, C.T., Gazirini, M.L., Beraldo, F.H., Varotti, F.P., Lopes, C., Markus, R.P., Pozzan, T., and Garcia, C.R. (2000). Calcium-dependent modulation by melatonin of the circadian rhythm in malarial parasites. *Nat. Cell Biol.* **2**, 466–468. <https://doi.org/10.1038/35017112>.
79. Prior, K.F., Rijo-Ferreira, F., Assis, P.A., Hirako, I.C., Weaver, D.R., Gazzinelli, R.T., and Reece, S.E. (2020). Periodic Parasites and Daily Host Rhythms. *Cell Host Microbe* **27**, 176–187. <https://doi.org/10.1016/j.chom.2020.01.005>.
80. Ramos, S., Ademolue, T.W., Jentho, E., Wu, Q., Guerra, J., Martins, R., Pires, G., Weis, S., Carlos, A.R., Mahú, I., et al. (2022). A hypometabolic defense strategy against malaria. *Cell Metabol.* **34**, 1183–1200.e12. <https://doi.org/10.1016/j.cmet.2022.06.011>.
81. Prior, K.F., Middleton, B., Owolabi, A.T.Y., Westwood, M.L., Holland, J., O'Donnell, A.J., Blackman, M.J., Skene, D.J., and Reece, S.E. (2021). Synchrony between daily rhythms of malaria parasites and hosts is driven by an essential amino acid. *Wellcome Open Res.* **6**, 186. <https://doi.org/10.12688/wellcomeopenres.16894.2>.
82. Kennaway, D.J. (2019). Melatonin research in mice: a review. *Chronobiol. Int.* **36**, 1167–1183. <https://doi.org/10.1080/07420528.2019.1624373>.
83. Subudhi, A.K., O'Donnell, A.J., Ramaprasad, A., Abkhallo, H.M., Kaushik, A., Ansari, H.R., Abdel-Haleem, A.M., Ben Rached, F., Kaneko, O., Culleton, R., et al. (2020). Malaria parasites regulate intra-erythrocytic development duration via serpentine receptor 10 to coordinate with host rhythms. *Nat. Commun.* **11**, 2763. <https://doi.org/10.1038/s41467-020-16593-y>.
84. Smith, L.M., Motta, F.C., Chopra, G., Moch, J.K., Nerem, R.R., Cummins, B., Roche, K.E., Kelliher, C.M., Leman, A.R., Harer, J., et al. (2020). An intrinsic oscillator drives the blood stage cycle of the malaria parasite

- Plasmodium falciparum*. *Science* 368, 754–759. <https://doi.org/10.1126/science.aba4357>.
85. Griffin, P., Dimitry, J.M., Sheehan, P.W., Lananna, B.V., Guo, C., Robinette, M.L., Hayes, M.E., Cedeño, M.R., Nadarajah, C.J., Ezerskiy, L.A., et al. (2019). Circadian clock protein Rev-erb α regulates neuroinflammation. *Proc. Natl. Acad. Sci. USA* 116, 5102–5107. <https://doi.org/10.1073/pnas.1812405116>.
 86. Briggs, J., Murray, M., Nideffer, J., and Jagannathan, P. (2023). Sex-Linked Differences in Malaria Risk Across the Lifespan. In *Sex and Gender Differences in Infection and Treatments for Infectious Diseases*, C.W. Roberts and S.L. Klein, eds. (Current Topics in Microbiology and Immunology), pp. 185–208.
 87. Klein, P.W., Easterbrook, J.D., Lalime, E.N., and Klein, S.L. (2008). Estrogen and progesterone affect responses to malaria infection in female C57BL/6 mice. *Genet. Med.* 5, 423–433. <https://doi.org/10.1016/j.genm.2008.10.001>.
 88. Vandermosten, L., Pham, T.T., Possemiers, H., Knoop, S., Van Herck, E., Deckers, J., Franke-Fayard, B., Lamb, T.J., Janse, C.J., Opendakker, G., and Van den Steen, P.E. (2018). Experimental malaria-associated acute respiratory distress syndrome is dependent on the parasite-host combination and coincides with normocyte invasion. *Malar. J.* 17, 102. <https://doi.org/10.1186/s12936-018-2251-3>.
 89. Carroll, R.W., Wainwright, M.S., Kim, K.Y., Kidambi, T., Gómez, N.D., Taylor, T., and Haldar, K. (2010). A rapid murine coma and behavior scale for quantitative assessment of murine cerebral malaria. *PLoS One* 5, e13124. <https://doi.org/10.1371/journal.pone.0013124>.
 90. Van Den Ham, K.M., Shio, M.T., Rainone, A., Fournier, S., Krawczyk, C.M., and Olivier, M. (2015). Iron prevents the development of experimental cerebral malaria by attenuating CXCR3-mediated T cell chemotaxis. *PLoS One* 10, e0118451. <https://doi.org/10.1371/journal.pone.0118451>.
 91. Van Den Ham, K.M., Smith, L.K., Richer, M.J., and Olivier, M. (2017). Protein Tyrosine Phosphatase Inhibition Prevents Experimental Cerebral Malaria by Precluding CXCR3 Expression on T Cells. *Sci. Rep.* 7, 5478. <https://doi.org/10.1038/s41598-017-05609-1>.

STAR★METHODS

KEY RESOURCES TABLE

REAGENT or RESOURCE	SOURCE	IDENTIFIER
Antibodies		
FITC anti-mouse CD4	Biologend	Cat#100405; RRID:AB_312691
APC/Cyanine7 anti-mouse CD8a	Biologend	Cat#100714; RRID:AB_312753
PE anti-mouse/human CD44	Biologend	Cat#103007; RRID:AB_493686
APC anti-mouse CD62L	Biologend	Cat#104411; RRID:AB_313098
PE/Cyanine7 anti-mouse CD45	Biologend	Cat#103113; RRID:AB_312979
BV421 rat anti-mouse TER-119/Erythroid Cells	BD Biosciences	Cat#563998; RRID:AB_2738534
APC rat anti-mouse CD71	BD Biosciences	Cat#567258; RRID:AB_2916520
PE anti-mouse/human CD44	Biologend	Cat#103023; RRID:AB_493686
Chemicals, peptides, and recombinant proteins		
Fetal Bovine Serum Heat-inactivated	Wisent Bioproduct	Cat#080-450
Sucrose	VWR	Cat#470302-810
Evans blue	Sigma-Aldrich	Cat#E2129
Critical commercial assays		
Kwik-Diff Staining Kit	ThermoFisher	Cat#9990700
Tekland Global 18% protein	Inotivco	Cat#2018
1x RBC Lysis Buffer	Biologend	Cat#420301
eBioscience Fixable Viability Dye eFluor 780	ThermoFisher	Cat#65-0865-14
Firefly Luciferase Assay Kit 2.0	Biotium	Cat#30085-T
Experimental models: Organisms/strains		
Mouse: C57BL/6N	Charles River Laboratories	RRID:MG1:2159965
Mouse: Rev-erba knockout: B6.Cg-Nr1d1 ^{tm1Ven} /LazJ	The Jackson Laboratory	RRID:IMSR_JAX:018447
<i>Plasmodium berghei</i> , strain ANKA 676m1cl1	Bei Resources	MRA-868
<i>Plasmodium chabaudi adami</i> DK	Provided by Dr. Mary Stevenson (McGill University, Canada)	N/A
Software and algorithms		
FlowJo software version 10.8.2	FlowJo, LLC	www.flowjo.com
Prism software version 9.3.1	GraphPad	www.graphpad.com
Other		
Mouse Cytokine Proinflammatory Focused 10-Plex Discovery Assay Array	Eve Technologies	MDF10
Contour NEXT EZ glucometer device	Ascensia	N/A

RESOURCE AVAILABILITY

Lead contact

Further information and requests for resources and reagents should be directed to and will be fulfilled by the lead contact, Nicolas Cermakian (nicolas.cermakian@mcgill.ca).

Materials availability

This study did not generate new unique reagents.

Data and code availability

- All data reported in this paper will be shared by the [lead contact](#) upon request.

- This paper does not report original code.
- Any additional information required to reanalyze the data reported in this paper is available from the [lead contact](#) upon request.

EXPERIMENTAL MODEL AND STUDY PARTICIPANT DETAILS

Mouse strains and housing conditions

C57BL/6N mice (RRID:MGI:2159965) were purchased from Charles River Laboratories (St-Constant, QC). *Rev-erba* knockout mice (B6.Cg-Nr1d1^{tm1Ven}/LazJ; RRID:IMSR_JAX:018447), were purchased from The Jackson Laboratory (# 018447, Bar Harbor, Maine, USA), and were bred in house at the Douglas Research Centre. All mice used for experiments were males, due to previous reports on lack of effect of sex on parasitemia or parasite load (although there can be sex differences in the immune response to the parasite^{87,88}). Mice were randomly assigned to experimental groups. Experimental animals were group-housed (3-5/cage) in light-proof ventilated cabinets (Actimetrics, Wilmette, IL, USA). Cabinet lighting was controlled via an external timer, with a light intensity of 150-200 lux (cool white LED lighting). Animal use was in accordance with the guidelines of the Canadian Council of Animal Care and was approved by the Douglas Institute Facility Animal Care Committee.

For time point experiments, mice were placed in cages under a standard 12 h light: 12 h dark (12:12 LD) cycle for 3 weeks (entrainment period) followed by *Plasmodium berghei* ANKA infection at the specified time points (mice were 8 weeks old at the time of infection). Mice were housed in different compartments of the cabinets, under different 12:12 LD cycles, such that all mice were infected at the same time, using the same batch of parasites. For circadian disruption experiments, mice (8 weeks old at the beginning of the jet lag procedure) were subjected to either a short-term circadian disruption protocol (6-h phase advance of the LD cycle every week, for a total of 4 weeks) or a chronic circadian disruption protocol (8-h phase advance of the LD cycle every 2 days, for a total of 10 weeks prior to infection). Mice of the control group remained on 12:12 LD for the entire duration of the experiment.

Plasmodium spp. strains

The parasites used in most experiments were *Plasmodium berghei*, strain ANKA 676m1c1 (MRA-868 Bei Resources). Some experiments were done with *Plasmodium chabaudi adami* DK, kindly provided by Dr. Mary Stevenson (McGill University, Canada).

METHOD DETAILS

Plasmodium spp. infections

Two mice were used as pass mice and injected intraperitoneally with either 10⁶ *Plasmodium berghei* ANKA-infected red blood cells (iRBCs) or 10⁶ *Plasmodium chabaudi adami*-infected RBCs. On day 6 post-infection, blood was collected from the pass mouse and the frequency of infected cells was measured by manual counting of blood smears stained with Kwik-Diff Staining Kit (ThermoFisher). The volume of blood collected from the pass mouse used to infect the experimental mice (10⁶ iRBCs/mouse) was calculated based on the frequency of infected cells obtained, and the number of erythrocytes/mL in the bloodstream (5 x 10⁹ erythrocytes/mL of blood). Experimental mice were infected via intraperitoneal injection at the time points indicated for each experiment.

Time-restricted feeding protocol

Mice were housed for 3 weeks under 12:12 LD with food and water *ad libitum*, followed by infection with 10⁶ iRBCs at Zeitgeber time (ZT) 7 (i.e. 7 h after lights on). Twenty-four hours after infection, mice were randomly assigned to an "ad libitum" group or a "time-restricted feeding" group. In the "ad libitum" group, food was given *ad libitum* (Tekland Global 18% protein). In the "time-restricted feeding" group, food was accessible only between ZT19 and ZT7 every day until day 4 post-infection inclusively.

Sucrose administration protocol

Mice were housed for 3 weeks under 12:12 LD with food and water *ad libitum*, followed by infection with 10⁶ iRBCs at ZT7. Twenty-four hours after infection, mice were randomly assigned to a "control" group or a "sucrose" group. In the "control" group, regular drinking water was given *ad libitum*. In the "sucrose" group, mice received regular water supplemented with 50% sucrose w/v daily, from ZT13 to ZT1, until day 4 post-infection inclusively (bottles with regular water without sucrose between ZT1 and ZT13). Water bottle rotation was also done for mice of the "control" group, for consistency.

Mouse survival and clinical scores

Mouse survival and clinical score were checked 3 times per day starting on day 4 post-infection. Clinical score was assessed using the Rapid Murine Coma and Behavior Scale (RMCBS)⁸⁹ based on 5 categories: coordination (gait, balance; max possible score: 4), exploratory behavior (motor performance; max possible score: 2), strength and tone (body position, limb strength; max possible score: 4), reflexes (touch scape, pinna reflex, toe pinch and aggression; max possible score: 8) and hygiene (grooming; max possible score: 2). Mice with a sum of the scores equal of below 15 (out of a maximum total of 20) were considered as under experimental cerebral malaria (ECM).

Blood-brain barrier integrity

The integrity of the blood-brain barrier was assessed by Evans blue dye incorporation in the brain tissue as previously described.⁹⁰ Briefly, mice received a single intraperitoneal injection of 0.3 mL of 2% Evans blue (Sigma-Aldrich) in PBS 1x. Mice were euthanized 2 h later, and brains were collected to verify the presence of the dye (qualitative assessment).

Flow cytometry

To study splenic T cells, on day 7 post-infection, mice were euthanized, spleens were collected and mechanically dissociated, and erythrocytes lysed using 1x RBC Lysis Buffer (Biolegend, #420301). Samples were centrifuged, and 5×10^6 cells per sample were resuspended in PBS 1x with 2% FBS. Cells were incubated with an antibody cocktail containing FITC anti-mouse CD4 (Biolegend, #100405), APC/Cyanine7 anti-mouse CD8a (Biolegend, #100714), PE anti-mouse/human CD44 (Biolegend, #103007) and APC anti-mouse CD62L (Biolegend, #104411) antibodies, for 30 minutes in the dark and on ice. Cells were washed and incubated in 1% PFA for 15 minutes on ice. Cells were washed, resuspended in PBS 1x with 2% FBS.

For reticulocytes assessment, on day 4 post-infection, 10 μ L of blood from ZT7- and ZT19-infected mice and their respective uninfected controls were collected (sampling time ZT7 or ZT19) and diluted in PBS 1x containing 20 U/mL of heparin, on ice. Animals were euthanized and spleens were collected, and mechanically dissociated. Blood and spleen samples were passed through a 0.40 μ m cell strainer, stained with trypan blue, and counted. Samples were centrifuged and 5×10^6 cells/sample were resuspended in PBS 1x with 2% FBS and stained with eBioscience Fixable Viability Dye eFluor 780 for 15 minutes followed by a washing step and incubation with anti-mouse CD16/32 antibody (Biolegend, #101319) for 15 minutes in the dark and on ice. Cells were then washed and incubated with an antibody cocktail containing PE/Cyanine7 anti-mouse CD45 (Biolegend, #103113), BV421 rat anti-mouse TER-119/Erythroid Cells (BD Biosciences, #563998), APC rat anti-mouse CD71 (BD Biosciences, #567258) and PE anti-mouse/human CD44 (Biolegend, #103023) antibodies for 30 minutes, in the dark and on ice. Cells were washed and incubated in PFA 1% for 5 minutes on ice. Cells were washed, resuspended in PBS 1x with 2% FBS. Cells were analyzed on the same day or following day using a FACS Canto II flow cytometer (BD Biosciences). Analysis was performed using FlowJo software version 10.8.2.

Parasitemia and parasite stage forms

The frequency of infected red blood cells (parasitemia) and the proportion of ring forms, trophozoites, schizonts and gametocytes (parasite stage forms) were assessed by tail tip blood collection as previously described.⁹¹ A blood smear was stained with Kwik-Diff Staining Kit (ThermoFisher) and by using an inverted microscope with 100X immersion oil objective, non-infected and infected red blood cells were counted (300 cells) and the percentage of parasite-containing cells was determined. Multi-infected (red blood cells with 2 or more parasites internalized) and single-infected RBCs (red blood cells with 1 parasite internalized) were also counted.

Parasite load (blood and organs)

The *P. berghei* ANKA parasite strain used in this study expresses luciferase. Based on this, parasite load was determined using the Firefly Luciferase Assay Kit 2.0 (Biotium). One microliter of blood was collected from the tail tip once a day starting day 4 post-infection. Blood was centrifuged and red blood cells were lysed using Lysis buffer 1x. For parasite organ sequestration, on day 7 post-infection, animals were euthanized by cervical dislocation and intracardially perfused with PBS 1x for 3 minutes. The liver, spleen, brain, and lungs were removed and mechanically processed in Lysis buffer 1x. Bioluminescence in the red blood cell extracts or in organ supernatants was measured using an Orion II Microplate Luminometer.

Cytokine/chemokine measurements

Blood from infected mice (ZT7 or ZT19) and their respective uninfected controls were collected using cardiac puncture (terminal) on day 7 post-infection. Blood was allowed to coagulate for 30 minutes prior to centrifugation at 500 g. Serum was collected and diluted 1:10 with sterile endotoxin-free PBS 1x. Aliquots were kept at -80°C and shipped on dry ice to Eve Technologies (Calgary, CA). Cytokine/chemokine levels were quantified using the Mouse Cytokine Proinflammatory Focused 10-Plex Discovery Assay Array (MDF10, Eve Technologies).

Glucose measurements

One microliter of blood was collected every 6 h (ZT1, 7, 13, 19) from tail tip from infected mice their respective uninfected controls, and plasma glucose was measured using Contour NEXT EZ glucometer device.

QUANTIFICATION AND STATISTICAL ANALYSIS

Statistical analyses were performed using GraphPad Prism software version 9.3.1. The data were expressed as mean \pm SEM. Circadian rhythmicity was evaluated by non-linear regression analysis (cosinor) by fitting a cosine wave equation $y = B + (A \cdot \cos(2 \cdot \pi \cdot ((x - Ps)/24)))$, where A = amplitude, B = baseline, Ps = phase shift, with a fixed period of 24 h. Significance was calculated based on F -value (observed R^2 , sample size and number of predictors). Survival analysis was performed by Log-rank (Mantel-Cox) analysis. Comparisons between 2 or more groups over time were done using mixed-effects model (REML) or two-way ANOVA with multiple comparisons test. Comparisons for 3 or more groups were performed using one-way ANOVA with multiple comparisons test. Comparisons between 2 groups were performed using Mann-Whitney test. All comparisons with p values <0.05 were considered significant. Detailed information of statistical analyses and group sizes are presented in figure legends.